

Nonsmooth Newton methods with effective subspaces for polyhedral regularization

TRAN T. A. NGHIA*

NGHIA V. VO[†]KHOA V. H. VU[‡]

Abstract

We propose several new nonsmooth Newton methods for solving convex composite optimization problems with polyhedral regularizers, while avoiding the computation of complicated second-order information on these functions. Under the tilt-stability condition at the optimal solution, these methods achieve the quadratic convergence rates expected of Newton schemes. Numerical experiments on Lasso, generalized Lasso, OSCAR-regularized least-square problems, and an image super-resolution task illustrate both the broad applicability and the accelerated convergence profile of the proposed algorithms, in comparison with first-order and several recently developed nonsmooth Newton schemes.

Mathematics Subject Classification (2020). 49J52, 49J53, 49M15, 65K10, 90C25

Keywords: Nonsmooth Newton methods, Polyhedral regularization, Generalized Hessian, Variational Analysis, Convex Optimization

1 Introduction

In this paper, we mainly design nonsmooth Newton methods for solving the following composite optimization problem

$$\min_{x \in \mathbb{X}} \quad \varphi(x) := f(x) + g(x), \quad (1.1)$$

where \mathbb{X} is a Euclidean space, $f : \mathbb{X} \rightarrow \mathbb{R}$ is a convex function that is continuously twice differentiable, and $g : \mathbb{X} \rightarrow \overline{\mathbb{R}} := \mathbb{R} \cup \{+\infty\}$ is a lower semicontinuous *polyhedral* (possibly nonsmooth) penalty function. Problems of the form (1.1) cover a broad variety of applications in machine learning, statistics, signal processing, image analysis, and optimal control. In this setting, one typically combines a data-fidelity term with a regularization term that encodes prior structural information on the solution.

To list a few important optimization problems of the format (1.1), we have the classical Least Absolute Shrinkage and Selection Operator [38] (in brief, Lasso) problem well-studied in statistics, signal processing, and sparse optimization, in which the nonsmooth regularizer is the ℓ_1 norm, $g(x) = \|x\|_1 = \sum_{i=1}^n |x_i|$, $x \in \mathbb{R}^n$, that is certainly a polyhedral convex function. The ℓ_1 regularizer is also used in different problems, including the ℓ_1 regularized logistic regression widely employed for binary classification and high-dimensional feature selections when the fidelity term $f(x)$ is the *logistic loss*. Another significant class of polyhedral regularizer is the *1D total variation*

*Department of Mathematics and Statistics, Oakland University, Rochester, MI 48309, USA; email: nt-tran@oakland.edu

[†]Department of Mathematics and Statistics, Oakland University, Rochester, MI 48309, USA; email: nghi-avo@oakland.edu

[‡]Department of Mathematics, Wayne State University, Detroit, MI 48202, USA; email: khoavu@wayne.edu

(TV) semi-norm defined by $g(x) = \sum_{i=1}^{n-1} |x_i - x_{i+1}|$, $x \in \mathbb{R}^n$, which promotes piecewise constant solutions and is significant in signal reconstruction. Beyond these classical examples, several structured polyhedral regularizers have been proposed to capture richer patterns. The fused Lasso [39] augments the ℓ_1 penalty with successive differences, $g(x) = \lambda_1 \|x\|_1 + \lambda_2 \sum_{i=1}^{n-1} |x_i - x_{i+1}|$ with parameters $\lambda_1, \lambda_2 > 0$, encouraging both sparsity and smoothness in ordered features such as time-series or genomic data. The clustered Lasso [37] penalizes pairwise differences between variables, $g(x) = \lambda_1 \|x\|_1 + \lambda_2 \sum_{i < j} |x_i - x_j|$, thereby promoting simultaneous sparsity and grouping of predictors with similar effects. The OSCAR penalty [6], $g(x) = \lambda_1 \|x\|_1 + \lambda_2 \sum_{i < j} \max\{|x_i|, |x_j|\}$, encourages both sparsity and grouping of predictors with equal magnitude. Finally, the $\ell_1 + \ell_\infty$ regularizer [40], $g(x) = \lambda_1 \|x\|_1 + \lambda_2 \|x\|_\infty$, induces structured sparsity by combining element-wise shrinkage with block-wise suppression.

With its wide range of applications, there are numerous iterative strategies for solving problem (1.1), which can be classified into first-order and second-order methods. Proximal first-order methods such as the Proximal Gradient Method (a.k.a. Iterative Shrinkage-Thresholding Algorithm (ISTA)), the Fast Proximal Gradient Method (a.k.a. Fast Iterative Shrinkage-Thresholding Algorithm (FISTA)), the Alternating Direction Method of Multipliers (ADMM), the Primal-Dual Algorithm, and their variants are the most widely used; see, e.g., [3, 7, 9] for a comprehensive analysis of these algorithms. They rely on inexpensive proximal mappings to handle the nonsmooth term g and enjoy global convergence guarantees with sublinear rates or linear rates under stronger assumptions on the model (1.1). Nevertheless, first-order methods may exhibit slow convergence in high-accuracy regimes. This motivates the development of Newton-type methods for solving (1.1) that can exploit second-order information and usually yield a faster convergence rate.

Adapting the original Newton method to nonsmooth composite optimization is highly non-trivial, since the classical Hessian is undefined on the nonsmooth function g . Several major approaches have emerged. *Semismooth* Newton methods in [25, 33, 12] exploit the semismoothness of proximal mappings and Clarke generalized derivatives, and have been widely applied to complementarity problems and variational inequalities. While effective, their local quadratic convergence analysis typically requires some special conditions that either fail in certain cases or hard to verify in practice. Moreover, finding one element of the Clarke generalized derivative can be a very difficult task in many complicated situations. A different line of work is the *coderivative-based* Newton methods recently developed in [31, 19, 18]; a systematic exposition can be found in [26, Chapter 9]. This framework also provides a natural extension of Newton steps by using the so-called *generalized Hessian* (a.k.a. the *second-order limiting subdifferential*) [27, 32] on the function g and the key notion of *semismoothness** introduced by Gfrerer and Outrata [15]. The complexity of superlinear convergence of these methods shows evidence of their efficiency in solving many optimization problems [19, 18]. However, computing the generalized Hessian explicitly is a challenge in practice that makes finding Newton directions based on these frameworks to be limited in some special and simple cases of g . Another direction has been developed recently in [13, 14, 15, 16] introducing the so-called *Subspace Containing Derivative* (SCD) Newton method, which instead extracts second-order information and some special subspaces from the *graphical derivative* of the subdifferential mapping ∂g . [16] showed that the SCD Newton method is a special case of the coderivative-based one, while the former is computationally simpler. Again, the superlinear convergence is obtained for this method under some reasonable local conditions at the optimal solutions. Impressive experiments for different frameworks related to ℓ_1 regularizers conducted in [13, 14] clearly show the power of this method. However, it seems that the computation of subspace containing derivatives on more complex regularizers g is still complicated and abstract. Another geometric perspective for nonsmooth Newton method for solving (1.1) for \mathcal{C}^2 -partly smooth regularizers is exemplified in [1, 21], where proximal-gradient iterations are accelerated by switching to Riemannian Newton

steps once the active manifold is identified. This approach yields quadratic local convergence but requires a relative-interior non-degeneracy condition to make the active manifold to be identified at those points close to the optimal solution in question. Unfortunately, this condition may not hold in certain cases.

Our contribution. In this paper, we develop Newton-type methods for problem (1.1) that are both theoretically rigorous and computationally implementable. Our proposed algorithms do not need to compute any second-order information on the regularizer g and exploit merely its first-order information. At each iteration, we construct an *effective subspace*, defined as the parallel space of the subdifferential of the conjugate penalty function, and restrict the Newton step to this subspace. In particular, our main Newton method is designed as follows.

Algorithm 1 Newton method with effective subspaces

Input: $x_0 \in \mathbb{X}, \eta > 0$.

- 1: Find $(y_k, z_k) \in \text{gph } \partial g$ satisfying

$$\|z_k - \bar{z}\| + \|y_k - \bar{x}\| \leq \eta \|x_k - \bar{x}\| \quad (1.2)$$

with $\bar{z} := -\nabla f(\bar{x})$.

- 2: Define the effective subspace $L_k := \text{par } \partial g^*(z_k)$ and find a Newton direction $d_k \in L_k$ solving the following quadratic optimization problem

$$\min_{d \in L_k} \frac{1}{2} \langle \nabla^2 f(y_k) d, d \rangle - \langle z_k + \nabla f(y_k), d \rangle.$$

- 3: Update $x_{k+1} = y_k - d_k$.
-

In this setup, \bar{x} is an optimal solution of (1.1) and ∂g stands for the convex subdifferential of g . The typical condition (1.2) originated in [15] gives us flexible choices of (y_k, z_k) without determining the specific η . For example, they can be chosen from the ISTA iterations (or FISTA iterations with some modifications); see, e.g., our Section 3 for further details. The main contribution in our paper is the Newton step of finding Newton direction d_k . The *effective subspace* L_k , which is the parallel space of the subdifferential of the conjugate function g^* at z_k , is computed only based on the first-order information. From the first sight, this step looks similar with the corresponding ones in [1, 21] with active manifolds and [13, 14] with subspaces containing derivative. However, even in the simple case of ℓ_1 regularizer, our effective subspaces are different from the active subspaces in [1, 21] that actually depend on y_k instead of z_k as designed in our algorithm. We will show later that our algorithm is a particular case of the SCD Newton method developed in [13, 14] and also the coderivative-based Newton method [18] for two special classes of regularizers at which g is either an indicator function or a support function of a polyhedral convex set. Nevertheless, we have an explicit formula of choosing the effective subspace L_k that is fully computable in many complex polyhedral regularizers aforementioned; see also Section 4 and 5 for further details.

Moreover, we prove that this scheme can achieve the quadratic convergence as desired for Newton methods without the non-degeneracy assumption in [1, 21], while other papers [13, 14, 15, 18, 19, 31] in this direction only obtain superlinear convergence for their Newton methods. Our analysis for quadratic convergence of our algorithm is grounded in the landmark notion of *tilt-stability* of minimizers introduced by Poliquin and Rockafellar [32], a concept that characterizes Lipschitz continuity of solution mapping via a *tilt/linear perturbation* on the objective function. In

convex settings, this condition at the minimizer \bar{x} is equivalent to some other conditions on (*strong*) *metric regularity* of the subdifferential mapping also used in [13, 18] for convergence analysis.

In our paper, an important part is the exact computation of the effective subspace L_k for several classes of polyhedral regularizers, including the support functions of convex sets containing many polyhedral (semi-)norms in \mathbb{R}^n such as the ℓ_1 norm, the ℓ_∞ norm, the sorted ℓ_1 norm and the 1D total variation semi-norm. We also obtain a general formula for computing this effective subspace of composite convex functions and apply it to evaluate the case of 1D total variation semi-norm mentioned above. Finally, we validate the theoretical findings with numerical experiments on synthetic and image datasets, showing that our Newton variants dramatically accelerate convergence for ISTA/FISTA and can outperform some other second-order algorithms such as those developed recently in [13, 19, 22] in solving several problems, including Lasso, ℓ_∞ -regularized problem, OSCAR, and 1D total variation problem.

2 Preliminaries

Throughout this paper, we denote by \mathbb{X} a finite-dimensional Euclidean space endowed with the inner product $\langle \cdot, \cdot \rangle$ and the corresponding Euclidean norm $\| \cdot \|$. For a subspace $S \subseteq \mathbb{X}$, P_S stands for the *orthogonal projection* onto S and S^\perp is the *orthogonal complement* of S . Given a nonempty set $C \subseteq \mathbb{X}$, the *span*, *affine hull*, *convex conic hull*, *convex hull*, and *closure* of C are denoted, respectively, by $\text{span } C$, $\text{aff } C$, $\text{cone } C$, $\text{conv } C$, and $\text{cl } C$. For a linear operator $A : \mathbb{X} \rightarrow \mathbb{Y}$, we write $\text{Ker } A$ and $\text{Im } A$, respectively, for the *kernel/null space* and *image/range* of A . The set $\mathbb{B}_\varepsilon(\bar{x})$ is the *closed ball* in \mathbb{X} centered at $\bar{x} \in \mathbb{X}$ with radius $\varepsilon > 0$.

2.1 Tools from Convex Analysis

Let C be a closed convex set in \mathbb{X} . The *support function* of C is given by

$$\sigma_C(v) := \sup_{x \in C} \langle v, x \rangle \quad \forall v \in \mathbb{X}. \quad (2.1)$$

The topological *relative interior* of C is the set

$$\text{ri } C := \{x \in \mathbb{X} \mid \exists \varepsilon > 0 : \mathbb{B}_\varepsilon(x) \cap \text{aff } C \subset C\}.$$

The *normal cone* to C at $x \in C$ is defined as

$$N_C(x) := \{v \in \mathbb{X} \mid \langle v, y - x \rangle \leq 0, \forall y \in C\}. \quad (2.2)$$

Let us recall the *tangent cone* to the convex set C at $x \in C$ here

$$T_C(x) := \text{cl}(\text{cone}(C - x)), \quad (2.3)$$

which is a closed convex cone. Indeed, the *polar* of the tangent cone $T_C(x)$ is the normal cone $N_C(x)$ defined above and vice versa due to the convexity of C .

One of the central definitions throughout the paper is the *parallel subspace* of $C \subseteq \mathbb{X}$, which is given by

$$\text{par } C := \text{span}(C - x) \quad \text{for all } x \in C. \quad (2.4)$$

Note that the parallel subspace of any convex cone $K \subset \mathbb{X}$ can be calculated as

$$\text{par } K = \text{span } K = K - K.$$

For a proper, lower semi-continuous (l.s.c), and convex function $\varphi : \mathbb{X} \rightarrow \overline{\mathbb{R}} = \mathbb{R} \cup \{+\infty\}$, the *effective domain* and the *epigraph* of φ are defined, respectively, by

$$\text{dom } \varphi := \{x \in \mathbb{X} \mid \varphi(x) < \infty\} \quad \text{and} \quad \text{epi } \varphi := \{(x, t) \in \mathbb{X} \times \mathbb{R} \mid \varphi(x) \leq t\}.$$

The *convex subdifferential* of φ at $x \in \text{dom } \varphi$ is known as

$$\partial\varphi(x) := \{v \in \mathbb{X} \mid \varphi(y) \geq \varphi(x) + \langle v, y - x \rangle, \forall y \in \mathbb{X}\}. \quad (2.5)$$

The normal cone $N_C(x)$ in (2.2) is indeed the subdifferential (2.5) of the *indicator function* $\delta_C(\cdot)$ at x , which is defined by $\delta_C(x) = 0$ whenever $x \in C$, and ∞ otherwise.

The *Legendre-Fenchel conjugate* of φ is the convex function $\varphi^* : \mathbb{X} \rightarrow \overline{\mathbb{R}}$ defined by

$$\varphi^*(v) := \sup_{x \in \mathbb{X}} \{\langle v, x \rangle - \varphi(x)\} \quad \text{for all } v \in \mathbb{X}.$$

When $\varphi(x) = \delta_C(x)$ is the indicator function to a convex set C , its conjugate δ_C^* is exactly the support function σ_C (2.1) to C .

A fundamental result in Convex Analysis is the Fenchel-Young's identity occasionally used in our paper, which states that

$$v \in \partial\varphi(x) \quad \text{if and only if} \quad \varphi(x) + \varphi^*(v) = \langle v, x \rangle. \quad (2.6)$$

Let us recall next the *proximal operator* of a convex function φ

$$\mathbf{prox}_{\alpha\varphi}(x) := \arg \min_{y \in \mathbb{X}} \left\{ \varphi(y) + \frac{1}{2\alpha} \|y - x\|^2 \right\} \quad \forall x \in \mathbb{X}, \forall \alpha > 0. \quad (2.7)$$

The proximal mapping $\mathbf{prox}_{\alpha\varphi} : \mathbb{X} \rightarrow \mathbb{X}$ associated with a convex function φ is a single-valued mapping with full domain. Moreover, it can be expressed equivalently as the *resolvent operator* $(\mathbb{I} + \alpha\partial\varphi)^{-1}$, where $\mathbb{I} : \mathbb{X} \rightarrow \mathbb{X}$ is the *identity operator*. Using the resolvent formula, we derive the following equivalence

$$y = \mathbf{prox}_{\alpha\varphi}(x) \quad \text{if and only if} \quad \frac{x - y}{\alpha} \in \partial\varphi(y). \quad (2.8)$$

2.2 Tools from Variational Analysis

In this section, we mainly follow the notations from the classical monographs [28, 26, 36] on Variational Analysis. Given a closed (possibly nonconvex) set $\Omega \subset \mathbb{X}$ and $\bar{x} \in \Omega$. The *regular normal cone* (a.k.a. Fréchet normal cone) to Ω at \bar{x} is defined by

$$\widehat{N}_\Omega(\bar{x}) := \left\{ v \in \mathbb{X} \mid \limsup_{x \xrightarrow{\Omega} \bar{x}} \frac{\langle v, x - \bar{x} \rangle}{\|x - \bar{x}\|} \leq 0 \right\},$$

where $x \xrightarrow{\Omega} \bar{x}$ means that $x \in \Omega$ and $x \rightarrow \bar{x}$. The *limiting normal cone* (a.k.a. Mordukhovich normal cone) to Ω at $\bar{x} \in \Omega$ is given by

$$N_\Omega(\bar{x}) := \{v \in \mathbb{X} \mid \exists \{x_k\} \xrightarrow{\Omega} \bar{x}, \{v_k\} \rightarrow v \text{ such that } v_k \in \widehat{N}_\Omega(x_k) \forall k \in \mathbb{N}\}. \quad (2.9)$$

Both the regular and limiting normal cones return exactly to the convex normal cone introduced in (2.2) when the set Ω is convex, but they are different in general.

For a set-valued mapping $F : \mathbb{X} \rightrightarrows \mathbb{X}$ from \mathbb{X} to itself, we associate with it the *graph* given by

$$\text{gph } F := \{(x, y) \in \mathbb{X} \times \mathbb{X} \mid y \in F(x)\}.$$

The *limiting coderivative* of a set-valued mapping $F : \mathbb{X} \rightrightarrows \mathbb{X}$ at $(\bar{x}, \bar{v}) \in \text{gph } F$ is defined as

$$D^*F(\bar{x}|\bar{v})(w) := \{z \in \mathbb{X} \mid (z, -w) \in N_{\text{gph } F}(\bar{x}, \bar{v})\} \quad \text{for all } w \in \mathbb{X}. \quad (2.10)$$

When F is the convex subdifferential mapping $\partial\varphi$ and $\bar{v} \in \partial\varphi(\bar{x})$, the limiting coderivative of $\partial\varphi$ at \bar{x} for \bar{v} is known as the *generalized Hessian* (a.k.a. *second-order limiting subdifferential*) [27, 28, 32] of φ at \bar{x} for \bar{v} denoted by:

$$\partial^2\varphi(\bar{x}|\bar{v})(w) := (D^*\partial\varphi)(\bar{x}|\bar{v})(w) \quad \text{for all } w \in \mathbb{X}, \quad (2.11)$$

which plays an important role in our paper and several nonsmooth Newton methods developed recently in [18, 19, 31]. It is worth noting that if φ is convex and twice continuously differentiable around \bar{x} with $\bar{v} = \nabla\varphi(\bar{x})$, then its generalized Hessian reduces to the regular Hessian mapping

$$\partial^2\varphi(\bar{x}|\bar{v})(w) = \nabla^2\varphi(\bar{x})w \quad \text{for all } w \in \mathbb{X}.$$

In this case, the classical Newton method for finding a minimizer \bar{x} of φ is designed as: Initiate $x_0 \in \mathbb{X}$ and proceed

$$x_{k+1} = x_k - d_k \quad \text{with } d_k := [\nabla^2\varphi(x_k)]^{-1}\nabla\varphi(x_k). \quad (2.12)$$

Since \bar{x} is a (local) minimizer of φ , the Hessian $\nabla^2\varphi(\bar{x})$ is always positive semi-definite. The existence of Newton direction d_k requires the Hessian $\nabla^2\varphi(x_k)$ to be non-singular. To make this happen, it is conventional to assume that the Hessian $\nabla^2\varphi(\bar{x})$ is positive definite and start with x_0 being sufficiently close to \bar{x} . When $\nabla^2\varphi(x)$ is Lipschitz continuous around \bar{x} , it is well-known that the above sequence $\{x_k\}$ converges *quadratically* to \bar{x} in the sense that there exists a constant $C > 0$ (independent of x_0) such that

$$\|x_{k+1} - \bar{x}\| \leq C\|x_k - \bar{x}\|^2 \quad \text{for any } k \in \mathbb{N}. \quad (2.13)$$

If φ is not twice differentiable, designing Newton methods is a huge challenge, as the regular Hessian does not exist anymore. Naturally, replacing the Hessian in (2.12) by the generalized Hessian (2.11) is a possibility; see, e.g., **Algorithm 2** and [31, 26, 19, 18]. Spontaneously, the generalized Hessian $\partial^2\varphi(\bar{x}|0)$ may need to be “positive definite” to match the classical theory. This actually leads us to the definition of *tilt stability* at a minimizer \bar{x} introduced by Poliquin and Rockafellar in [32], which is shown to be equivalent to the positive definiteness of $\partial^2\varphi(\bar{x}|0)$; see [32, Theorem 1.3] or Theorem 2.2 below. It is worth mentioning that the general definition and theory of tilt stability [32, 26] is for nonconvex and nonsmooth functions; here, we slightly modify it for the convex case.

Definition 2.1 (Tilt stability). *Given an l.s.c. convex function $\varphi : \mathbb{X} \rightarrow \overline{\mathbb{R}}$, a point $\bar{x} \in \text{dom } \varphi$ is called a tilt stable minimizer of φ if there exists $\gamma > 0$ such that the mapping*

$$M_\gamma(v) := \arg \min\{\varphi(x) - \langle v, x \rangle \mid x \in \mathbb{B}_\gamma(\bar{x})\} \quad \text{for } v \in \mathbb{X}$$

is single-valued and Lipschitz continuous on some neighborhood of $0 \in \mathbb{X}$ with $M_\gamma(0) = \{\bar{x}\}$.

Tilt-stability also lies behind the theory of nonsmooth Newton methods developed recently in [31, 19, 13]. The following theorem, a direct consequence of [29, Theorem 3.5] and [36, Example 13.30], gives a complete characterization of tilt stability and will be useful for our later analysis.

Theorem 2.2. (A characterization of tilt stability via generalized Hessian) *Consider an l.s.c. convex function $\varphi : \mathbb{X} \rightarrow \overline{\mathbb{R}}$ with $\bar{x} \in \text{dom } \varphi$ and $0 \in \partial\varphi(\bar{x})$. Then \bar{x} is a tilt stable minimizer of φ if and only if the generalized Hessian $\partial^2\varphi$ is positive definite around $(\bar{x}, 0)$ in the sense that there exist $\kappa, r > 0$ satisfying*

$$\langle z, w \rangle \geq \kappa \|w\|^2 \quad \forall z \in \partial^2\varphi(x|v)(w), \quad \forall (x, v) \in \mathbb{B}_r(\bar{x}, 0) \cap \text{gph } \partial\varphi. \quad (2.14)$$

3 Newton methods with effective subspaces polyhedral regularization

In this section, we propose some nonsmooth Newton methods for solving the following composite optimization problem

$$\min_{x \in \mathbb{X}} \quad \varphi(x) := f(x) + g(x), \quad (3.1)$$

where $f : \mathbb{X} \rightarrow \mathbb{R}$ is a convex function that is twice continuously differentiable and $g : \mathbb{X} \rightarrow \overline{\mathbb{R}}$ is a proper piecewise linear/polyhedral convex function. Recall that a proper function g is piecewise linear/polyhedral and convex if and only if its epigraph is *polyhedral*, i.e., it is the intersection of finitely many closed half-spaces in $\mathbb{X} \times \mathbb{R}$ [36, Definition 2.47 and Theorem 2.49].

Suppose that \bar{x} is an optimal solution of problem (3.1). To motivate our algorithm, let us recall the following coderivative-based Newton methods in [18, Algorithm 1 and Algorithm 2] below.

Algorithm 2 The coderivative-based Newton method

Input: $x_0 \in \mathbb{X}, \eta > 0$.

1: Find $(y_k, z_k) \in \text{gph } \partial g$ satisfying

$$\|z_k - \bar{z}\| + \|y_k - \bar{x}\| \leq \eta \|x_k - \bar{x}\|, \quad (3.2)$$

where $\bar{z} := -\nabla f(\bar{x})$.

2: Find a Newton direction $d_k \in \mathbb{X}$ satisfying

$$-\nabla^2 f(y_k)d_k + z_k + \nabla f(y_k) \in \partial^2 g(y_k|z_k)(d_k). \quad (3.3)$$

3: Update $x_{k+1} = y_k - d_k$.

When $g \equiv 0$, we may choose $\eta = 1$, $y_k = x_k$, and $z_k = \bar{z} = 0$ to make (3.2) holds. In this case, inclusion (3.3) reduces exactly to the original Newton step in (2.12)

$$\nabla^2 f(x_k)d_k = \nabla f(x_k). \quad (3.4)$$

Thus, **Algorithm 2** is a natural extension of the classical Newton method (2.12) to problem (3.1), at which the second-order information of the nonsmooth function g is also involved via the generalized Hessian $\partial^2 g(y_k|z_k)$ in (3.3); see also [26, Chapter 9] for further history and state-of-art of this algorithm. For the general problem (3.1), the *approximation step* of finding $(y_k, z_k) \in \text{gph } \partial g$ satisfying (3.2) was initiated in [15] and used recently for several Newton methods in [13, 14, 18, 19]. We may choose the pair

$$y_k = \text{prox}_{\alpha g}(x_k - \alpha \nabla f(x_k)) \quad \text{and} \quad z_k = \frac{x_k - y_k}{\alpha} - \nabla f(x_k) \quad \text{with some} \quad \alpha > 0 \quad (3.5)$$

from the proximal gradient method [3] to satisfy this condition; see, e.g., [14, 18].

The generalized Newton step (3.3) has some roots in [31] and has been fully developed in the recent paper [18]. In particular, [18, Theorem 3.11 and Theorem 4.10] show that if the subdifferential mapping $\partial\varphi$ is *metrically regular* at the optimal solution \bar{x} of problem (3.1) for 0 in the sense of [11, Section 3E] and ∂g is *semismooth** at $(\bar{x}, -\nabla f(\bar{x}))$ in the sense of [15, Definition 3.1], then the sequence $\{x_k\}$ converges *superlinearly* to \bar{x} , i.e.,

$$\lim_{k \rightarrow \infty} \frac{\|x_{k+1} - \bar{x}\|}{\|x_k - \bar{x}\|} = 0,$$

provided that the initial x_0 is close enough to \bar{x} . The results in [18] work for more general frameworks at which the functions f and g do not need to be convex. For our convex setting in (3.1), the aforementioned metric regularity condition on the subdifferential mapping $\partial\varphi$ at \bar{x} for 0 is equivalent to the tilt-stability of φ at the minimizer \bar{x} in Definition 2.1. Moreover, the subdifferential mapping ∂g of our convex polyhedral function g is also a particular class of semismooth* multifunctions [16, Proposition 2.10].

The main challenge for **Algorithm 2** lies in the computation of the generalized Hessian in practice. Moreover, finding a Newton direction satisfying the inclusion in (3.3) seems to be a very nontrivial step. To address these issues, we propose a simple way of finding such d_k without computing the generalized Hessian of g . Motivated by the classical Newton step in (3.4), a solution d_k of the following system

$$-\nabla^2 f(y_k)d_k + z_k + \nabla f(y_k) = 0 \quad \text{and} \quad 0 \in \partial^2 g(y_k|z_k)(d_k) \quad (3.6)$$

satisfies (3.3) obviously. As g is a polyhedral function, so is its Legendre-Fenchel conjugate g^* . It follows from [30, Equation (4.9)] that

$$0 \in \partial^2 g(y_k|z_k)(d_k) \quad \text{if and only if} \quad d_k \in \partial^2 g^*(z_k|y_k)(0) = \text{par } \partial g^*(z_k), \quad (3.7)$$

which is the parallel space of $\partial g^*(z_k)$. This subspace is referred to as the *effective subspace* of g at y_k for z_k in our Newton methods. It actually signifies the null/kernel space of the generalized Hessian of g at y_k for $z_k \in \partial g(y_k)$. The system (3.6) turns into a linear system

$$-\nabla^2 f(y_k)d_k + z_k + \nabla f(y_k) = 0 \quad \text{and} \quad d_k \in L_k := \text{par } \partial g^*(z_k),$$

which has a solution when $\nabla^2 f(y_k)(L_k) = \mathbb{X}$. This condition may fail, leading to the above linear system may have no solution. As $\nabla^2 f(y_k)$ is positive semidefinite, the first equation hints us that d_k is a solution of the following quadratic optimization problem

$$\min_{d \in \mathbb{X}} \frac{1}{2} \langle \nabla^2 f(y_k)d, d \rangle - \langle z_k + \nabla f(y_k), d \rangle.$$

Since we also need the solution d_k to belong to the subspace L_k as in (3.6), we slightly modify the above optimization problem to

$$\min_{d \in L_k} \frac{1}{2} \langle \nabla^2 f(y_k)d, d \rangle - \langle z_k + \nabla f(y_k), d \rangle, \quad (3.8)$$

which means that d_k is a solution to the following linear system (instead of the proposed system (3.6))

$$-\nabla^2 f(y_k)d_k + z_k + \nabla f(y_k) \in L_k^\perp \quad \text{and} \quad d_k \in L_k. \quad (3.9)$$

Indeed, we show later that this system has a unique solution when x_0 is close to the tilt stable minimizer \bar{x} . These discussions motivate us to design our Newton method with effective subspaces L_k mentioned in the Introduction.

Algorithm 1: Newton method with effective subspaces

Input: $x_0 \in \mathbb{X}, \eta > 0$.

- 1: Find $(y_k, z_k) \in \text{gph } \partial g$ satisfying (3.2).
 - 2: Define the effective subspace $L_k := \text{par } \partial g^*(z_k)$ and find an optimal solution $d_k \in L_k$ of problem (3.8).
 - 3: Update $x_{k+1} = y_k - d_k$.
-

In Corollary 3.6, when g is either the indicator or the support function of a polyhedral convex set, we show that our Newton step (3.8) or (3.9) is indeed a particular case of (3.3) and the recent Newton method [14, Algorithm 4.2] that uses the so-called *Subspace Containing* (SC) derivative of the subdifferential mapping ∂g , which is also a second-order structure. The idea of using effective subspaces to find a Newton direction in (3.8) is also close to the latter. However, comparing with other algorithms established recently, it seems that our effective subspaces L_k have more explicit and computable settings. Most importantly, with these effective subspaces, we are able to prove next that **Algorithm 1** acquires quadratic convergence around the tilt stable minimizer \bar{x} , which is the desirable complexity for Newton methods instead of superlinear convergence obtained in [14, 18]. Although our **Algorithm 1** is influenced by other Newton methods in [14, 18], the proof of our main result for the quadratic convergence of **Algorithm 1** is completely different.

Before proceeding to the main theorem, let us recall the recent result in [10, Theorem 4.3] stating that \bar{x} is a tilt stable minimizer of φ in our setting (3.1) if and only if $-\nabla f(\bar{x}) \in \partial g(\bar{x})$ and

$$\text{Ker } \nabla^2 f(\bar{x}) \cap \text{par } \partial g^*(-\nabla f(\bar{x})) = \{0\}, \quad (3.10)$$

which is rather simple to check at \bar{x} via linear algebra. The appearance of the effective subspace $\text{par } \partial g^*(-\nabla f(\bar{x}))$ in this characterization also serves as another motivation for our **Algorithm 1** above.

Theorem 3.1 (Quadratic convergence of the Newton method with effective subspaces). *Consider problem (3.1) in which $f : \mathbb{X} \rightarrow \mathbb{R}$ is a twice continuously differentiable and convex function and $g : \mathbb{X} \rightarrow \overline{\mathbb{R}}$ is a convex polyhedral function. Suppose that \bar{x} is a tilt stable minimizer of the function φ in (3.1), i.e., $-\nabla f(\bar{x}) \in \partial g(\bar{x})$ and condition (3.10) holds, and that the Hessian $\nabla^2 f(x)$ is Lipschitz continuous around \bar{x} . Then there exists $\varepsilon > 0$ such that for any starting point $x_0 \in \mathbb{B}_\varepsilon(\bar{x})$, we have the assertions:*

- (i) *The optimal solution $\{d_k\}$ of problem (3.8) is well-defined and unique.*
- (ii) *The sequence $\{x_k\}$ generated by **Algorithm 1** converges quadratically to \bar{x} .*

Proof. Since \bar{x} is a tilt stable local minimizer to problem (3.1), the characterization from (2.14) holds with respect to some constants $\kappa, r > 0$. Further, we may shrink r if needed so that there exists $\ell > 0$ satisfying

$$\begin{aligned} \langle z, w \rangle &\geq \kappa \|w\|^2 \quad \forall z \in \partial^2 \varphi(x|v)(w), \quad \forall (x, v) \in \text{gph } \partial \varphi \cap \mathbb{B}_r(\bar{x}, 0), \\ \|\nabla f(x) - \nabla f(\bar{x})\| &\leq \ell \|x - \bar{x}\|, \quad \forall x \in \mathbb{B}_r(\bar{x}), \\ \|\nabla^2 f(x) - \nabla^2 f(y)\| &\leq \ell \|x - y\|, \quad \forall x, y \in \mathbb{B}_r(\bar{x}). \end{aligned} \quad (3.11)$$

Let us pick a universal constant $0 < \varepsilon < \min \left\{ \frac{r}{2\eta(1+\ell)}; \frac{\kappa}{\ell\eta^2} \right\}$ and set $\bar{C} := \frac{\ell\eta^2}{2\kappa}$. By the choice of ε , it follows that $2\bar{C}\varepsilon < 1$.

We claim **(i)** and **(ii)** by induction as follows. Supposing $x_k \in \mathbb{B}_\varepsilon(\bar{x})$ for some $k \in \mathbb{N} \cup \{0\}$, we will show that the optimal solution d_k to problem (3.8) exists uniquely and the inequalities $\|x_{k+1} - \bar{x}\| \leq \bar{C}\|x_k - \bar{x}\|^2 < \varepsilon$ hold. First, observe from step 1 in **Algorithm 1** that

$$\|y_k - \bar{x}\| \leq \eta\|x_k - \bar{x}\| \leq \eta\varepsilon < \frac{r}{2}. \quad (3.12)$$

Define $v_k := \nabla f(y_k) + z_k \in \partial\varphi(y_k)$. We obtain from (3.2) that

$$\|v_k\| = \|\nabla f(y_k) - \nabla f(\bar{x}) + z_k - \bar{z}\| \leq \ell\|y_k - \bar{x}\| + \|z_k - \bar{z}\| \leq (1+\ell)\eta\varepsilon < \frac{r}{2}. \quad (3.13)$$

One gets from the first inequality of (3.11) at $(x, v) = (y_k, v_k) \in \text{gph } \partial\varphi \cap \mathbb{B}_r(\bar{x}, 0)$ due to (3.12)-(3.13) and the sum rule for the generalized Hessian [28, Proposition 1.121] that

$$\langle \nabla^2 f(y_k)w, w \rangle + \langle u, w \rangle \geq \kappa\|w\|^2 \quad \text{for all } u \in \partial^2 g(y_k|z_k)(w).$$

By choosing $u = 0$, the latter inequality together with the identity from (3.7) gives us that

$$\langle \nabla^2 f(y_k)w, w \rangle \geq \kappa\|w\|^2 \quad \text{for all } w \in L_k = \text{par } \partial g^*(z_k), \quad (3.14)$$

which means $\nabla^2 f(y_k)$ is positive definite over L_k . This guarantees the uniqueness of the optimal solution d_k of the quadratic optimization problem (3.8).

Next, let us verify the estimates $\|x_{k+1} - \bar{x}\| \leq \bar{C}\|x_k - \bar{x}\|^2 < \varepsilon$. To proceed, by using the variational geometry of convex polyhedral sets given in [11, Theorem 2E.3], we may shrink $r > 0$ if needed so that the continuity of g relative to its domain deduces the relation

$$T_{\text{epi } g}(x, g(x)) \supset T_{\text{epi } g}(\bar{x}, g(\bar{x})) \quad \text{for any } x \in \text{dom } g \cap \mathbb{B}_r(\bar{x})$$

via the tangent cone in (2.3). Then, the polarity between the normal cone and tangent cone to convex sets yields

$$N_{\text{epi } g}(x, g(x)) \subset N_{\text{epi } g}(\bar{x}, g(\bar{x})),$$

which further ensures that

$$\partial g(x) \subset \partial g(\bar{x}) \quad \text{for any } x \in \text{dom } g \cap \mathbb{B}_r(\bar{x}).$$

It follows from (3.12) that

$$z_k \in \partial g(y_k) \subset \partial g(\bar{x}),$$

which implies that $\bar{x}, y_k \in \partial g^*(z_k)$. Consequently, we derive that

$$x_{k+1} - \bar{x} = y_k - d_k - \bar{x} \in \text{span}(\partial g^*(z_k) - \bar{x}) = L_k. \quad (3.15)$$

By (3.9), we may write

$$\nabla^2 f(y_k)d_k = z_k + \nabla f(y_k) - e_k \quad \text{for some } e_k \in L_k^\perp. \quad (3.16)$$

Employing (3.16) gives us that

$$\begin{aligned} \nabla^2 f(y_k)(x_{k+1} - \bar{x}) &= \nabla^2 f(y_k)(y_k - \bar{x}) - \nabla^2 f(y_k)d_k \\ &= \nabla^2 f(y_k)(y_k - \bar{x}) - z_k - \nabla f(y_k) + e_k \\ &= \nabla^2 f(y_k)(y_k - \bar{x}) + \nabla f(\bar{x}) - \nabla f(y_k) - (z_k - \bar{z}) + e_k. \end{aligned} \quad (3.17)$$

We claim next that

$$P_{L_k}(z_k - \bar{z}) = 0. \quad (3.18)$$

Since $\text{epi } g$ is a convex polyhedral set in $\mathbb{X} \times \mathbb{R}$, the Reduction Lemma from [11, Lemma 2E.4] lends us a neighborhood $U \times V$ of $(0, 0) \in (\mathbb{X} \times \mathbb{R})^2$, independent of k , on which the identity

$$(U \times V) \cap (\text{gph } N_{\text{epi } g} - (\bar{x}, g(\bar{x}), \bar{z}, -1)) = (U \times V) \cap \text{gph } N_K \quad (3.19)$$

holds, where $K := T_{\text{epi } g}(\bar{x}, g(\bar{x})) \cap \{(\bar{z}, -1)\}^\perp$ is known as the *critical cone* to $\text{epi } g$ at $(\bar{x}, g(\bar{x}))$ for $(\bar{z}, -1)$. Let us shrink $r > 0$ if necessary so that $\mathbb{B}_r(0) \subset V$, which yields $(z_k - \bar{z}, 0) \in V$ by (3.2). As g is continuous on its domain, there exists some fixed number $\mu_k > 0$ such that for any $y \in \partial g^*(z_k) \cap \mathbb{B}_{\mu_k}(\bar{x})$, we have $(y, g(y)) \in (\bar{x}, g(\bar{x})) + U$. It follows that

$$(y - \bar{x}, g(y) - g(\bar{x}), z_k - \bar{z}, 0) \in (U \times V) \cap (\text{gph } N_{\text{epi } g} - (\bar{x}, g(\bar{x}), \bar{z}, -1)),$$

which yields further by (3.19) the relationship

$$(z_k - \bar{z}, 0) \in N_K(y - \bar{x}, g(y) - g(\bar{x})).$$

Since K is a closed convex cone, this tells us that

$$\langle z_k - \bar{z}, y - \bar{x} \rangle = \langle z_k - \bar{z}, y - \bar{x} \rangle + 0 \cdot (g(y) - g(\bar{x})) = 0. \quad (3.20)$$

Hence, we have $z_k - \bar{z} \perp (\partial g^*(z_k) - \bar{x}) \cap \mathbb{B}_{\mu_k}(0)$, which yields

$$z_k - \bar{z} \perp \text{span}((\partial g^*(z_k) - \bar{x}) \cap \mathbb{B}_{\mu_k}(0)) = \text{span}(\partial g^*(z_k) - \bar{x}) = L_k,$$

where the last equality holds due to the fact that $\bar{x} \in \partial g^*(z_k)$. Our claim (3.18) is verified.

From (3.17) and (3.18), we have

$$P_{L_k}(\nabla^2 f(y_k)(x_{k+1} - \bar{x})) = P_{L_k}(\nabla^2 f(y_k)(y_k - \bar{x}) + \nabla f(\bar{x}) - \nabla f(y_k)),$$

which thus implies by the local Lipschitz continuity of $\nabla^2 f$ around \bar{x} and (3.11)-(3.12) that

$$\begin{aligned} \|P_{L_k}(\nabla^2 f(y_k)(x_{k+1} - \bar{x}))\| &\leq \|\nabla^2 f(y_k)(y_k - \bar{x}) + \nabla f(\bar{x}) - \nabla f(y_k)\| \\ &= \left\| \int_0^1 [\nabla^2 f(y_k) - \nabla^2 f(y_k + t(\bar{x} - y_k))] (y_k - \bar{x}) dt \right\| \\ &\leq \int_0^1 \|\nabla^2 f(y_k) - \nabla^2 f(y_k + t(\bar{x} - y_k))\| \|y_k - \bar{x}\| dt \\ &\leq \frac{\ell}{2} \|y_k - \bar{x}\|^2. \end{aligned} \quad (3.21)$$

In addition, note from (3.15) that $x_{k+1} - \bar{x} \in L_k$. Applying (3.14) with $w = x_{k+1} - \bar{x} \in L_k$ gives us that

$$\langle \nabla^2 f(y_k)(x_{k+1} - \bar{x}), x_{k+1} - \bar{x} \rangle \geq \kappa \|x_{k+1} - \bar{x}\|^2,$$

which by the fact $x_{k+1} - \bar{x} \in L_k$ and the self-adjoint property of P_{L_k} is equivalent to

$$\langle P_{L_k}(\nabla^2 f(y_k)(x_{k+1} - \bar{x})), x_{k+1} - \bar{x} \rangle \geq \kappa \|x_{k+1} - \bar{x}\|^2.$$

The Cauchy-Schwarz's inequality then deduces

$$\|P_{L_k}(\nabla^2 f(y_k)(x_{k+1} - \bar{x}))\| \geq \kappa \|x_{k+1} - \bar{x}\|. \quad (3.22)$$

Combining (3.12), (3.21) and (3.22) with the choice of ε gives us

$$\|x_{k+1} - \bar{x}\| \leq \frac{\ell}{2\kappa} \|y_k - \bar{x}\|^2 \leq \frac{\ell\eta^2}{2\kappa} \|x_k - \bar{x}\|^2 = \bar{C} \|x_k - \bar{x}\|^2 \leq \frac{1}{2} \|x_k - \bar{x}\| < \varepsilon.$$

This justifies our inductive step and thus yields for each $k \in \mathbb{N} \cup \{0\}$ the optimal solution d_k of (3.8) together with the estimate $\|x_{k+1} - \bar{x}\| \leq \bar{C} \|x_k - \bar{x}\|^2$, where \bar{C} is independent of k . The assertions in (i) and (ii) are thus justified. \square

Remark 3.2. In the proof of our main Theorem 3.1, the polyhedrality of g plays an essential role, whereas the function f does not need to be convex. Tilt stability at \bar{x} leads to (3.14), which guarantees the positive definiteness of $\nabla^2 f(y_k)$ on L_k and the uniqueness of the Newton direction d_k solving (3.8). However, to be consistent with our later applications as well as the developments for ISTA and FISTA in [3, 8], which we will use for the approximation step (3.2), and to avoid additional technical details, we still keep the assumption that f is convex throughout the paper.

As discussed after Algorithm 2, a practical way to choose $(y_k, z_k) \in \text{gph } \partial g$ satisfying (3.2) is using the proximal gradient (a.k.a. ISTA) step as in (3.5). We incorporate this step into our Algorithm 1 as follows and prove the corresponding quadratic convergence result for the sake of completeness.

Algorithm 3 ISTA-Newton method with effective subspaces

Input: $x_0 \in \mathbb{X}, \alpha > 0$.

- 1: Compute $y_k := \mathbf{prox}_{\alpha g}(x_k - \alpha \nabla f(x_k))$.
- 2: Compute $z_k := \frac{x_k - y_k}{\alpha} - \nabla f(x_k)$.
- 3: Compute $L_k := \text{par } \partial g^*(z_k)$ and find an optimal solution d_k of

$$\min_{d \in L_k} \frac{1}{2} \langle \nabla^2 f(y_k) d, d \rangle - \langle z_k + \nabla f(y_k), d \rangle.$$

- 4: Update $x_{k+1} = y_k - d_k$.
-

Corollary 3.3 (Quadratic convergence of the ISTA-Newton method with effective subspaces). *Under the assumptions of Theorem 3.1, there exists $\varepsilon > 0$ such that for each $x_0 \in \mathbb{B}_\varepsilon(\bar{x})$, Algorithm 3 produces a sequence $\{x_k\}$ converging quadratically to \bar{x} .*

Proof. The algorithm starts with some parameter $\alpha > 0$. To ensure the quadratic convergence via the proof by induction in Theorem 3.1, it suffices to show the fulfillment of our boundedness condition (3.2) at each pair $(y_k, z_k) \in \text{gph } \partial g$ ($k = 0, 1, \dots$), given that $x_k \in \mathbb{B}_\varepsilon(\bar{x})$. Indeed, Algorithm 3 forces $z_k \in \partial g(y_k)$ due to (2.8). Let us set

$$\eta := \frac{(2 + \alpha)(1 + \ell\alpha)}{\alpha}, \tag{3.23}$$

where ℓ is a Lipschitz modulus of ∇f around \bar{x} . Pick $x_k \in \mathbb{B}_\varepsilon(\bar{x})$, where ε is chosen as in Theorem 3.1, satisfying in addition $\varepsilon < r$ from (3.11). The *nonexpansiveness* property of $\mathbf{prox}_{\alpha g}$ implies that

$$\begin{aligned} \|y_k - \bar{x}\| &= \left\| \mathbf{prox}_{\alpha g}(x_k - \alpha \nabla f(x_k)) - \mathbf{prox}_{\alpha g}(\bar{x} - \alpha \nabla f(\bar{x})) \right\| \\ &\leq \left\| (x_k - \bar{x}) - \alpha (\nabla f(x_k) - \nabla f(\bar{x})) \right\| \leq (1 + \ell\alpha) \|x_k - \bar{x}\|. \end{aligned} \tag{3.24}$$

Moreover, it follows from (3.24) and the Lipschitz continuity of ∇f on $\mathbb{B}_\varepsilon(\bar{x})$ that

$$\|z_k - \bar{z}\| = \left\| \frac{x_k - y_k}{\alpha} - \nabla f(x_k) + \nabla f(\bar{x}) \right\| \leq \frac{\|x_k - \bar{x}\|}{\alpha} + \frac{\|y_k - \bar{x}\|}{\alpha} + \ell \|x_k - \bar{x}\|,$$

which together with (3.24) and (3.23) verifies (3.2) at the pair (y_k, z_k) . Our conclusion then follows from the inductive step as in the proof of Theorem 3.1. \square

Remark 3.4. (Comparisons with active submanifolds Newton methods in [1, 21, 41]) Compared to the Newton method with active Riemannian submanifolds built in [1, Algorithm 1 & 2] which also achieves quadratic convergence, our convergence theory does not require the often-assumed *non-degeneracy condition* $-\nabla f(\bar{x}) \in \text{ri } \partial g(\bar{x})$ in [1, Definition 3.2]. The latter property, which is indispensable in their construction named *r-structure critical point* \bar{x} , is used to determine a manifold \mathcal{M} such that the function g is \mathcal{C}^2 on \mathcal{M} and that x_k belongs to \mathcal{M} for sufficiently large k . However, this condition is not always true, as shown in the following example.

On $\mathbb{X} = \mathbb{R}^2$, consider the functions

$$f(x_1, x_2) := \frac{1}{2} \|(x_1, x_2) - (2, -1)\|^2 \quad \text{and} \quad g(x_1, x_2) := |x_1| + |x_2|, \quad \text{for} \quad (x_1, x_2) \in \mathbb{R}^2.$$

Note that $\nabla f(1, 0) = (-1, 1)$ and $\partial g(1, 0) = \{1\} \times [-1, 1]$. Hence, $\bar{x} := (1, 0)$ is a local minimizer of $f + g$, as it satisfies the first-order optimality condition $0 \in \nabla f(\bar{x}) + \partial g(\bar{x})$. Moreover, since $f + g$ is strongly convex, \bar{x} is a tilt stable minimizer to $f + g$. By performing as in **Algorithm 1** with a starting point close enough to \bar{x} , our iterates converge quadratically to \bar{x} , as a result of Theorem 3.1. However, observe that

$$-\nabla f(\bar{x}) = (1, -1) \notin \{1\} \times (-1, 1) = \text{ri } \partial g(\bar{x}),$$

i.e., the non-degeneracy condition is violated at \bar{x} .

Note further that in the setting of [1, Example 2.3], their *optimal submanifold* for this example is $\mathcal{M} = \mathbb{R} \times \{0\}$. From the first sight, it may be natural to think this submanifold is the effective subspace $L := \text{par } \partial g^*(-\nabla f(\bar{x}))$ in our approach. However, they are not the same, as

$$\text{par } \partial g^*(-\nabla f(\bar{x})) = \text{par} (N_{\mathbb{B}_\infty}(1, -1)) = \text{par} (\mathbb{R}_+ \times \mathbb{R}_-) = \mathbb{R}^2,$$

where \mathbb{B}_∞ is the ℓ_∞ norm unit ball in \mathbb{R}^2 . Moreover, the ℓ_1 norm $g(x)$ is not smooth on L . This somewhat distinguishes our algorithms from those in [1, 21, 41]. More specifically, for solving the more general optimization problem (3.1) with $g(x) = \|x\|_1$ in \mathbb{R}^n , the update of the active submanifold (subspace) at iteration k in [1, Example 2.3] and [41, Page 97] only relies on y_k as follows

$$\mathcal{M}_k = \{x \in \mathbb{R}^n \mid x_i = 0 \text{ for } i \in I_k\} \quad \text{with} \quad I_k := \{i \in \{1, \dots, n\} \mid (y_k)_i = 0\}.$$

This is usually referred as the *active subspace/submanifold* as it is built up based on the *active set* at y_k . However, our effective subspace L_k used to update Newton direction d_k in (3.3) relies on $z_k \in \partial g(y_k)$ as

$$L_k = \text{par} (N_{\mathbb{B}_\infty}(z_k)) = \{x \in \mathbb{R}^n \mid x_j = 0 \text{ for } j \in J_k\} \quad \text{with} \quad J_k := \{j \in \{1, \dots, n\} \mid |(z_k)_j| < 1\};$$

see also formula (4.2) in Section 4. Note that $J_k \subset I_k$ and therefore our effective subspaces L_k are larger than \mathcal{M}_k . Moreover, the ℓ_1 norm may not be smooth on L_k . In practice, it seems that the performance of **Algorithm 1** differs only slightly between these two updates when solving the ℓ_1 regularized optimization problems. However, as described above, we are able to prove the quadratic

convergence of **Algorithm 1** with our effective subspaces L_k without the non-degeneracy condition in [1, 21, 41]. More importantly, a closed-form computation of our effective subspaces L_k can be obtained explicitly by employing only the first-order information from g^* for any polyhedral function g ; see also Section 4 for explicit computations of other polyhedral regularizers. \square

Next, we establish several connections between our strategy of determining Newton directions with other nonsmooth Newton schemes developed recently in [13, 14, 15, 16, 18, 19, 31] for the special case when $g(x)$ is either the indicator or support function to a polyhedral set.

Proposition 3.5. Let C be a polyhedral convex set in \mathbb{X} . Suppose that g is either the indicator function δ_C or the support function σ_C . With $(\bar{x}, \bar{z}) \in \text{gph } \partial g$ and $L = \text{par } \partial g^*(\bar{z})$, there holds

$$L^\perp \times L \subset N_{\text{gph } \partial g}(\bar{x}, \bar{z}). \quad (3.25)$$

Moreover, we also have

$$L \times L^\perp \in \mathcal{S}\partial g(\bar{x}, \bar{z}), \quad (3.26)$$

where $\mathcal{S}\partial g$ is the *SC derivative* [16, Definition 3.3] of the subdifferential mapping ∂g .

Proof. Case I: $g(x) = \delta_C(x)$, the indicator function of C . Denote by

$$K := K_C(\bar{x}, \bar{z}) = T_C(\bar{x}) \cap \{\bar{z}\}^\perp \quad (3.27)$$

the critical cone of C at \bar{x} for \bar{z} . Recall that a cone F in \mathbb{X} is called a *closed face* of K if there exists some v in K^* , the polar cone of K , such that $F = K \cap \{v\}^\perp$. The limiting normal cone to $\text{gph } \partial g$ at (\bar{x}, \bar{z}) is expressed by [32, Proposition 4.4]

$$N_{\text{gph } \partial g}(\bar{x}, \bar{z}) = \{(F_1 - F_2)^* \times (F_1 - F_2) \mid F_1, F_2 \text{ are closed faces of } K \text{ with } F_2 \subset F_1\}. \quad (3.28)$$

As $L = \{w \mid (0, w) \in N_{\text{gph } \partial g}(\bar{x}, \bar{z})\}$ by (3.7) and $0 \in (F_1 - F_2)^*$ for any choice of closed faces F_1, F_2 of K in the above formula, we have

$$L = \bigcup \{F_1 - F_2 \mid F_1, F_2 \text{ are closed faces of } K \text{ with } F_2 \subset F_1\}.$$

As $F_1 - F_2 \subset K - K$ for any pair of closed faces F_1, F_2 of K , and a particular choice is $F_1 = F_2 = K$, the above identity gives us $L = K - K$. This together with (3.28) verifies (3.25).

To justify (3.26), let us recall the formula in [16, Equation (29) in Example 3.29] that

$$\mathcal{S}\partial g(\bar{x}, \bar{z}) = \mathcal{S}N_C(\bar{x}, \bar{z}) = \{(F - F) \times (F - F)^\perp \mid F \text{ is a closed face of } K\}. \quad (3.29)$$

As $L = K - K$, we obtain (3.26) immediately by choosing $F = K$ from the above formula.

Case II. $g(x) = \sigma_C(x) = \delta_C^*(x)$. In this case, $L = \text{par } \partial \delta_C(\bar{z}) = \text{par } N_C(\bar{z})$. Since $\partial g^* = (\partial g)^{-1}$, to justify (3.25), we just need to show that

$$L \times L^\perp \subset N_{\text{gph } \partial g^*}(\bar{z}, \bar{x}) = N_{\text{gph } N_C}(\bar{z}, \bar{x}). \quad (3.30)$$

The critical cone in this case has to be adjusted to $H = T_C(\bar{z}) \cap \{\bar{x}\}^\perp$. We claim next that $(\text{par } N_C(\bar{z}))^\perp$ is a closed face of H . Suppose that C can be represented by

$$C = \{z \in \mathbb{X} \mid \langle a_i, z \rangle \leq b_i, i = 1, \dots, n\}.$$

With $\bar{z} \in C$, we have

$$N_C(\bar{z}) = \text{cone } \{a_i \mid i \in I(\bar{z})\} \quad \text{with} \quad I(\bar{z}) := \{i \in \{1, \dots, n\} \mid \langle a_i, \bar{z} \rangle = b_i\}.$$

Obviously, $\text{span } N_C(\bar{z}) = \text{span } \{a_i \mid i \in I(\bar{z})\}$. Moreover, the tangent cone to C at \bar{z} is computed by

$$T_C(\bar{z}) = \{d \in \mathbb{X} \mid \langle a_i, d \rangle \leq 0, i \in I(\bar{z})\}.$$

As $\bar{x} \in N_C(\bar{z})$, we may write

$$\bar{x} = \sum_{i \in J} \lambda_i a_i$$

for some index set $J \subset I(\bar{z})$ with $\lambda_i > 0, i \in J$. Thus, the critical cone is obtained by

$$H = T_C(\bar{z}) \cap \{\bar{x}\}^\perp = \{d \in \mathbb{X} \mid \langle a_i, d \rangle = 0, i \in J, \langle a_i, d \rangle \leq 0, i \in I(\bar{z}) \setminus J\}.$$

Define $u := \sum_{i \in I(\bar{z}) \setminus J} a_i$ if $J \neq I(\bar{z})$ and $u := 0$ if $J = I(\bar{z})$. Note that $u \in H^*$ and that the closed face $F_1 := H \cap \{u\}^\perp$ is computed by

$$\begin{aligned} F_1 &= \{d \in \mathbb{X} \mid \langle a_i, d \rangle = 0, i \in J, \langle a_i, d \rangle \leq 0, i \in I(\bar{z}) \setminus J, \sum_{i \in I(\bar{z}) \setminus J} \langle a_i, d \rangle = 0\} \\ &= \{d \in \mathbb{X} \mid \langle a_i, d \rangle = 0, i \in J, \langle a_i, d \rangle = 0, i \in I(\bar{z}) \setminus J\}, \end{aligned}$$

which is exactly $(\text{par } N_C(\bar{z}))^\perp$. Combining this with the formula (3.28) with $F_2 = 0$ (but replacing (\bar{x}, \bar{z}) there with (\bar{z}, \bar{x}) and K with H) gives us that

$$L \times L^\perp = (\text{par } N_C(\bar{z}))^{\perp\perp} \times (\text{par } N_C(\bar{z}))^\perp \subset N_{\text{gph } \partial g^*}(\bar{z}, \bar{x}),$$

which is exactly (3.30). Hence, we also have (3.25) by interchanging the roles of L and L^\perp from $N_{\text{gph } \partial g^*}(\bar{z}, \bar{x})$ to $N_{\text{gph } \partial g}(\bar{x}, \bar{z})$. The inclusion (3.26) is derived similarly by replacing formula (3.28) with (3.29). \square

Corollary 3.6. Consider problem (3.1) in which g is either the indicator function or the support function of a polyhedral set in \mathbb{X} . **Algorithm 3** is a special case of **Algorithm 2** and [14, Algorithm 4.2].

Proof. Proceeding as in **Algorithm 3**, at each iteration, d_k solves the following linear system:

$$-\nabla^2 f(y_k) d_k + z_k + \nabla f(y_k) \in L_k^\perp \quad \text{and} \quad d_k \in L_k.$$

On the one hand, by using (3.25), we get

$$\left(-\nabla^2 f(y_k) d_k + z_k + \nabla f(y_k), -d_k \right) \in L_k^\perp \times L_k \subset N_{\text{gph } \partial g}(y_k, z_k),$$

which thus implies by (2.10) and (2.11) that $-\nabla^2 f(y_k) d_k + z_k + \nabla f(y_k) \in \partial^2 g(y_k | z_k)(d_k)$. This shows that our Newton step d_k satisfies the coderivative inclusion (3.3) from **Algorithm 2**.

On the other hand, employing (3.26) also indicates that our $-d_k$ can be chosen as a Newton direction in [14, Algorithm 4.2]. \square

Remark 3.7. Corollary 3.6 shows that when g is either the indicator or the support function of a convex polyhedral set in \mathbb{X} , our Newton scheme provides an efficient way of choosing Newton directions that are special instances of the coderivative-based [18] and the SCD Newton method [14, Algorithm 4.2] while avoiding computing any second-order structures of the regularizer g . In contrast to these approaches, which, under their standing assumptions, guarantee at most local superlinear convergence, our method uses only first-order information from the conjugate g^* yet still attains quadratic convergence. The trade-off is that our current theory applies only to convex piecewise linear/polyhedral functions g . \square

It is worth noticing that, in practice, the proximal gradient (ISTA) step may produce only small improvements in the early iterations. To make the algorithm faster, an accelerated version known as Fast Proximal Gradient Method (a.k.a. *Fast Iterative Shrinkage-Thresholding Algorithm* (FISTA)) [3, 8] is usually applied. In practice, since we do not know how to choose x_0 close to \bar{x} as required in Theorem 3.1, using FISTA may move the iterates quickly to a neighborhood of \bar{x} and then allow us to start the Newton step, which exhibits quadratic convergence. We modify **Algorithm 3** using FISTA below.

Algorithm 4 FISTA-Newton method with effective subspaces

Input: $x_0 = x_{-1} \in \mathbb{X}, \alpha > 0, \{\beta_k\} \subset (0, 1]$.

- 1: Compute $u_k := x_k + \beta_k(x_k - x_{k-1})$.
 - 2: Compute $y_k := \mathbf{prox}_{\alpha g}(u_k - \alpha \nabla f(u_k))$.
 - 3: Compute $z_k := \frac{u_k - y_k}{\alpha} - \nabla f(u_k)$.
 - 4: Compute $L_k := \text{par } \partial g^*(z_k)$ and find d_k solving problem (3.8).
 - 5: Update $x_{k+1} = y_k - d_k$.
-

Here, $\{\beta_k\}$ is a bounded below sequence in $(0, 1]$; see [3, 8, 23] for different ways of updating this sequence. We remark that the practice of combining FISTA with a second-order method for the ℓ_1 logistic regression problem appeared in [41, Page 99-100], where promising numerical performance was reported. However, the convergence analysis of this combined method is not provided there. In the following corollary, we establish a definitive convergence result for FISTA when employed within our effective subspace framework.

Unlike the scheme with ISTA-Newton update for (y_k, z_k) that satisfies (3.2) immediately, it is not clear to us if the choice of (y_k, z_k) in **Algorithm 4** also fulfills this condition because of the extrapolation step above, which involves both x_k and x_{k-1} . However, it is similar to (3.2) proved in Corollary 3.3 that

$$\begin{aligned} \|y_k - \bar{x}\| + \|z_k - \bar{z}\| &\leq \eta \|u_k - \bar{x}\| \\ &= \eta \|(1 + \beta_k)(x_k - \bar{x}) - \beta_k(x_{k-1} - \bar{x})\| \\ &\leq 2\eta \max\{\|x_k - \bar{x}\|; \|x_{k-1} - \bar{x}\|\} \end{aligned} \quad (3.31)$$

with $\eta > 0$ in (3.23). In order to prove the local quadratic convergence of this algorithm, we have to adjust our proof of Theorem 3.1 with the bound in (3.31) above.

Corollary 3.8 (Quadratic convergence-type of the FISTA-Newton method with effective subspaces). *Under the assumptions of Theorem 3.1, there exist $\varepsilon > 0$ and $\tilde{C} > 0$ (independent of ε) such that for each starting point $x_0 \in \mathbb{B}_\varepsilon(\bar{x})$, **Algorithm 4** produces a sequence $\{p_k\}$ defined by*

$$p_k := \max\{\|x_k - \bar{x}\|; \|x_{k-1} - \bar{x}\|\} \quad \text{for } k = 0, 1, \dots, \quad (3.32)$$

satisfying

- (i) $p_0, p_1 \leq \varepsilon$.
- (ii) $p_{k+2} \leq \tilde{C} p_k^2$ for all $k \in \mathbb{N} \cup \{0\}$.

Proof. The proof is slightly modified from the one for Theorem 3.1. Let us recall all the constants from (3.11) and define $\tilde{C} := \frac{2\ell\eta^2}{\kappa}$, with $\eta > 0$ taken from (3.23). Then choose $\varepsilon > 0$ satisfying

$$0 < \varepsilon < \min\left\{1; \frac{1}{\tilde{C}}; \frac{r}{4\eta}\right\}. \quad (3.33)$$

By induction, suppose that $p_k = \max \{ \|x_k - \bar{x}\|; \|x_{k-1} - \bar{x}\| \} \leq \varepsilon$ for some $k \in \mathbb{N} \cup \{0\}$, e.g., $p_0 \leq \varepsilon$. We claim that (3.8) has a unique optimal solution d_k and there hold the estimates $p_{k+1} \leq \varepsilon$ and $p_{k+2} \leq \tilde{C}p_k^2$. By (3.31), we have

$$\|y_k - \bar{x}\| + \|z_k - \bar{z}\| \leq 2\eta p_k \leq 2\eta\varepsilon \leq \frac{r}{2},$$

where η is taken from (3.23). Similarly to the proof of Theorem 3.1 after (3.12), the Newton step (3.8) also admits a unique solution d_k and

$$\|x_{k+1} - \bar{x}\| \leq \frac{\ell}{2\kappa} \|y_k - \bar{x}\|^2 \leq \tilde{C}p_k^2 \leq \tilde{C}\varepsilon^2 < \varepsilon, \quad (3.34)$$

which yields $p_{k+1} \leq \varepsilon$, as $\|x_k - \bar{x}\| \leq p_k \leq \varepsilon$. The upper bound estimate $p_{k+1} \leq \varepsilon$ is enough to guarantee $(y_{k+1}, z_{k+1}) \in \mathbb{B}_{\frac{r}{2}}(\bar{x}, \bar{z})$ due to (3.31), which again allows us to obtain

$$\|x_{k+2} - \bar{x}\| \leq \tilde{C}p_{k+1}^2. \quad (3.35)$$

Combining (3.34) and (3.35) gives us that

$$\begin{aligned} \|x_{k+2} - \bar{x}\| &\leq \tilde{C} \max \{ \|x_{k+1} - \bar{x}\|^2; \|x_k - \bar{x}\|^2 \} \leq \tilde{C} \max \{ \tilde{C}^2 \|x_k - \bar{x}\|^4; \tilde{C}^2 \|x_{k-1} - \bar{x}\|^4; \|x_k - \bar{x}\|^2 \} \\ &\leq \tilde{C} \max \{ \|x_k - \bar{x}\|^2; \|x_{k-1} - \bar{x}\|^2 \} = \tilde{C}p_k^2, \end{aligned}$$

where the last inequality is due to $\tilde{C}^2 p_k^2 = \tilde{C}^2 \max \{ \|x_k - \bar{x}\|^2; \|x_{k-1} - \bar{x}\|^2 \} \leq \tilde{C}^2 \varepsilon^2 < 1$. We derive from the above inequality and (3.34) that

$$p_{k+2} \leq \tilde{C}p_k^2$$

as claimed. This completes the proof of the corollary. \square

Remark 3.9 (Efficient extrapolation parameters in Algorithm 4). To the best of our knowledge, convergence of the iterates generated by the original FISTA in [3] has not been established. However, to accelerate convergence while ensuring that the iterates approach \bar{x} , we must guarantee that the sequence itself converges. This motivates the use of extrapolation schemes for which convergence of the iterates can be rigorously proved.

Several choices of the extrapolation parameters $\{\beta_k\}$ ensuring convergence of the sequence have been studied in the literature [8, 23], without assuming that \bar{x} is a tilt-stable minimizer. In particular, [23] proved the convergence of FISTA iterates under the parameterization

$$\beta_k = \frac{t_{k-1} - 1}{t_k}, \quad t_k = \frac{p + \sqrt{q + 4t_{k-1}^2}}{2}, \quad (3.36)$$

where $p \in (0, 1)$, $q \in [p^2, (2-p)^2]$ are tunable parameters controlling the growth of $\{\beta_k\}$.

An alternative choice was proposed in the Chambolle–Dossal variant of FISTA [8], where

$$\beta_k = \frac{k-1}{k+d}, \quad t_k = \frac{k+d}{d}, \quad d > 2. \quad (3.37)$$

This rule preserves the $O(1/k^2)$ convergence rate in terms of function values while guaranteeing convergence of the iterates. In practice, both parameterizations yield trajectories that are smoother and more stable than those of the original FISTA, which often exhibits oscillatory behavior. Consequently, these variants typically achieve comparable or improved overall performance, especially on ill-conditioned problems.

4 Effective subspaces of several polyhedral regularizers

In our **Algorithm 1**, the appearance of the effective subspace $L_k = \text{par } \partial g^*(z_k)$ plays a crucial role. In this section, we illustrate concretely how these subspaces are computed in some specific polyhedral convex regularizers $g(x)$ broadly used in optimization and machine learning problems. These computations will be employed later in Section 5, when we experiment the performance of our **Algorithms 3 and 4** for different optimization models.

Proposition 4.1 (Support functions). *Suppose that $g = \sigma_C : \mathbb{X} \rightarrow \overline{\mathbb{R}}$ is the support function of a closed convex set C . Then $\text{par } \partial g^*(z) = \text{span } N_C(z)$ for any $z \in C$.*

Proof. As $g(x) = \sigma_C(x)$, we have $g^* = \delta_C$, the indicator function to C . It follows that $\partial g^*(z) = N_C(z)$. As $N_C(z)$ is a closed convex cone in \mathbb{X} , we have

$$\text{par } \partial g^*(z) = N_C(z) - N_C(z) = \text{span } N_C(z).$$

The proof is complete. □

Any norm in \mathbb{X} can be represented as the support function of its *dual unit ball*. Particularly, we consider the case of ℓ_1 norm, its variant known as sorted ℓ_1 norm, and ℓ_∞ norm below.

(i) ℓ_1 norm. Let $g(x) := \sum_{i=1}^n |x_i|$ for $x \in \mathbb{R}^n$. We have

$$g^* = (\|\cdot\|_1)^* = (\sigma_{\mathbb{B}_\infty})^* = \delta_{\mathbb{B}_\infty}, \quad (4.1)$$

where $\mathbb{B}_\infty = \{v \in \mathbb{R}^n \mid |v_i| \leq 1, i = 1, \dots, n\}$ is the ℓ_∞ unit ball in \mathbb{R}^n . For any $z \in \mathbb{B}_\infty$, it is well-known that

$$\partial g^*(z) = N_{\mathbb{B}_\infty}(z) = \left\{ x \in \mathbb{R}^n \mid \begin{cases} x_i = 0 & \text{if } |z_i| < 1 \\ x_i z_i \geq 0 & \text{if } |z_i| = 1 \end{cases} \right\}.$$

Hence, we have

$$\text{par } \partial g^*(z) = N_{\mathbb{B}_\infty}(z) - N_{\mathbb{B}_\infty}(z) = \{x \in \mathbb{R}^n \mid x_i = 0 \text{ if } |z_i| < 1\} = \{0\}^{J(z)} \times \mathbb{R}^{J(z)^c}, \quad (4.2)$$

where $J(z) := \{i \in \{1, \dots, n\} \mid |z_i| < 1\}$.

(ii) ℓ_∞ norm. When g is the ℓ_∞ norm, in the manner of (4.1) we have

$$g^* = (\|\cdot\|_\infty)^* = (\sigma_{\mathbb{B}_{\|\cdot\|_1}})^* = \delta_{\mathbb{B}_{\|\cdot\|_1}},$$

where $\mathbb{B}_{\|\cdot\|_1} := \{v \in \mathbb{R}^n \mid \|v\|_1 \leq 1\}$ is the ℓ_1 unit ball. It follows that $\partial g^*(z) = N_{\mathbb{B}_{\|\cdot\|_1}}(z)$ for each $z \in \mathbb{R}^n$. It follows from Proposition 4.1 that

$$\text{par } \partial g^*(z) = \text{span } (N_{\mathbb{B}_{\|\cdot\|_1}}(z)). \quad (4.3)$$

Throughout this section, we use the *sign function* as follows:

$$\text{sign}(\alpha) := \begin{cases} 1 & \text{if } \alpha > 0 \\ -1 & \text{if } \alpha < 0 \\ 0 & \text{if } \alpha = 0 \end{cases} \quad \text{for any } \alpha \in \mathbb{R}.$$

Moreover, define $\text{sign}(z) := (\text{sign}(z_i))_{1 \leq i \leq n}$ for any $z \in \mathbb{R}^n$. According to the formula of normal cone to a lower level-set [36, Proposition 10.3], we have

$$N_{\mathbb{B}_{\|\cdot\|_1}}(z) = \text{cone}(\partial\|\cdot\|_1(z)) = \text{cone} \left\{ x \in \mathbb{R}^n \mid \begin{cases} x_i \in [-1, 1] & \text{if } z_i = 0 \\ x_i = \text{sign}(z_i) & \text{if } z_i \neq 0 \end{cases} \right\}. \quad (4.4)$$

Combining (4.4) with (4.3) yields the inclusion

$$\text{par } \partial g^*(z) \subset \{x \in \mathbb{R}^n \mid \exists \alpha \in \mathbb{R} : x_i = \alpha \text{sign}(z_i) \text{ if } z_i \neq 0\} = \mathbb{R}^{I(z)} \times \mathbb{R}(\text{sign}(z_i))_{i \notin I(z)}, \quad (4.5)$$

where $I(z) := \{i \mid z_i = 0\}$. To justify the opposite inclusion to (4.5), pick $x \in \mathbb{R}^n$ such that there exists $\alpha \in \mathbb{R}$ satisfying $x_i = \alpha \text{sign}(z_i)$ for each $i \notin I(z)$. With $\alpha^+ := \max\{0, \alpha\}$ and $\alpha^- := \max\{0, -\alpha\}$, let $p, q \in \mathbb{R}^n$ with coordinates given by

$$(p_i, q_i) := \begin{cases} (x_i, 0) & \text{if } z_i = 0, \\ \left(\sum_{j \in I(z)} |x_j| + \alpha^+, \sum_{j \in I(z)} |x_j| + \alpha^- \right) & \text{if } z_i > 0, \\ - \left(\sum_{j \in I(z)} |x_j| + \alpha^+, \sum_{j \in I(z)} |x_j| + \alpha^- \right) & \text{if } z_i < 0, \end{cases} \quad \text{for } i = 1, \dots, n.$$

Observe from (4.4) that $p, q \in N_{\mathbb{B}_{\|\cdot\|_1}}(z)$ and $x = p - q$. Consequently, the opposite inclusion to (4.5) holds. Hence, we have

$$\text{par } \partial g^*(z) = \mathbb{R}^{I(z)} \times \mathbb{R}(\text{sign}(z_i))_{i \notin I(z)}. \quad (4.6)$$

(iii) Sorted ℓ_1 norm. For any vector $x \in \mathbb{R}^n$, denote by $|x|_{(i)}$ the i^{th} largest absolute value among coordinates of x , with ties distributed by an arbitrary rule. In the Sorted L-One Penalized Estimation (SLOPE) model (see, e.g., [24]), the sorted ℓ_1 norm is defined by

$$g(x) := \sum_{i=1}^n \lambda_i |x|_{(i)} \quad \text{for } x \in \mathbb{R}^n, \quad (4.7)$$

with parameters $\lambda_1 \geq \lambda_2 \geq \dots \geq \lambda_n \geq 0$ and $\lambda_1 > 0$. Note that the OSCAR model [6] is a special case of SLOPE, by choosing $\lambda_i := w_1 + w_2(n - i)$, $i = 1, \dots, n$ with parameters $w_1, w_2 \geq 0$.

From [24, Section 4], we know that g^* is the indicator function to the following convex set

$$C_\lambda := \left\{ z \in \mathbb{R}^n \mid \sum_{i=1}^k |z|_{(i)} \leq \sum_{i=1}^k \lambda_i \text{ for each } k \in \{1, \dots, n\} \right\}. \quad (4.8)$$

Hence, $\partial g^* = N_{C_\lambda}$. By letting $s_k(z) := \sum_{i=1}^k |z|_{(i)}$ and $\Lambda_k := \sum_{i=1}^k \lambda_i$, we rewrite C_λ as

$$C_\lambda = \bigcap_{k=1}^n \{z \in \mathbb{R}^n \mid s_k(z) \leq \Lambda_k\},$$

i.e., C_λ is an intersection of finitely many lower level-sets. As $\lambda_1 > 0$, we have $\Lambda_k > 0$ for any $k \in \{1, \dots, n\}$. Thus the Slater's condition for C_λ holds at the origin. It follows from the Kuhn-Tucker theorem (see, e.g., [35, Corollary 28.3.1]) that $N_{C_\lambda}(z)$ is exactly the convex conic hull of subgradients corresponding to the active constraints at z , i.e., one has

$$N_{C_\lambda}(z) = \text{cone} \left(\bigcup_{k \in A(z)} \partial s_k(z) \right) \quad \text{with } A(z) := \{k \in \{1, \dots, n\} \mid s_k(z) = \Lambda_k\}. \quad (4.9)$$

By Proposition 4.1, $\text{par } \partial g^*(z) = \text{span } N_{C_\lambda}(z)$. To construct this subspace, we need to compute $\partial s_k(z)$.

Proposition 4.2 (Subdifferential of $s_k(z)$). *For any $z \in \text{dom } g^*$ with g being the sorted ℓ_1 norm defined in (4.7) and for any $k \in A(z)$, define the following index sets*

$$T_k := \{i \mid |z_i| > |z|_{(k)}\}, \quad E_k := \{i \mid |z_i| = |z|_{(k)}\}, \quad \text{and} \quad R_k := \{i \mid |z_i| < |z|_{(k)}\}.$$

We have

$$\partial s_k(z) = \begin{cases} \left\{ v \in \mathbb{B}_\infty \mid \|v\|_1 \leq k \text{ and } v_i = \text{sign}(z_i) \text{ if } i \in T_k \right\} & \text{if } |z|_{(k)} = 0 \\ \left\{ v \in \mathbb{B}_\infty \mid v_i \in \begin{cases} \{\text{sign}(z_i)\} & \text{if } i \in T_k \\ \mathbb{R}_+ \text{sign}(z_i) & \text{if } i \in E_k \\ \{0\} & \text{if } i \in R_k \end{cases} \text{ and } \sum_{i \in E_k} |v_i| = k - |T_k| \right\} & \text{if } |z|_{(k)} > 0, \end{cases}$$

where $|T_k|$ denotes the cardinality of the set T_k . Consequently, it follows that

$$\text{span } \partial s_k(z) = \begin{cases} \text{span} \left\{ v_k, (e_j)_{j \in E_k} \right\} & \text{if } |z|_{(k)} = 0 \\ \text{span} \left\{ v_k, \left(e_j - \frac{\text{sign}(z_j)}{\text{sign}(z_{m_k})} e_{m_k} \right)_{j \in E_k \setminus \{m_k\}} \right\} & \text{if } |z|_{(k)} > 0, \end{cases}$$

where v_k is any subgradient in $\partial s_k(z)$ determined above, $e_j := (0, \dots, 0, 1, 0, \dots, 0)^T$ is the j^{th} unit vector in \mathbb{R}^n , and m_k is the largest index in E_k . These formulas for $k \in A(z)$ provide us a spanning set for the parallel space $\text{par } \partial g^*(z)$ as follows

$$\text{par } \partial g^*(z) = \text{span} \left(\bigcup_{k \in A(z)} \text{span}(\partial s_k(z)) \right). \quad (4.10)$$

Proof. First, let us claim that

$$s_k(z) = \max_{\|v\|_\infty \leq 1, \|v\|_1 \leq k} \langle v, z \rangle. \quad (4.11)$$

Indeed, observe that $s_k(z) = \sum_{i=1}^k |z|_{(i)} = \langle \bar{v}, z \rangle$ with $\bar{v} \in \mathbb{R}^n$ given by

$$\bar{v}_i = \begin{cases} \text{sign}(z_i) & \text{if } i \in T_k \\ \alpha_i \text{sign}(z_i) & \text{if } i \in E_k \\ 0 & \text{if } i \in R_k \end{cases} \quad \text{with } \alpha_i \geq 0, i \in E_k \text{ and } \sum_{i \in E_k} \alpha_i = k - |T_k|.$$

As $\|\bar{v}\|_\infty \leq 1$ and $\|\bar{v}\|_1 \leq k$, we obviously have the inequality “ \leq ” in (4.11). Regarding the opposite inequality, for each $v \in \mathbb{R}^n$ with $\|v\|_\infty \leq 1$ and $\|v\|_1 \leq k$, there hold the estimates

$$\begin{aligned} s_k(z) - \langle v, z \rangle &\geq \sum_{i=1}^k |z|_{(i)} - \sum_{i=1}^n |v_i| |z_i| \\ &= \sum_{i \in T_k} (1 - |v_i|) |z_i| + \left(k - |T_k| - \sum_{i \in E_k} |v_i| \right) |z|_{(k)} - \sum_{i \in R_k} |v_i| |z_i| \\ &= \sum_{i \in T_k} (1 - |v_i|) (|z_i| - |z|_{(k)}) + \left(k - \sum_{i=1}^n |v_i| \right) |z|_{(k)} + \sum_{i \in R_k} |v_i| (|z|_{(k)} - |z_i|) \\ &\geq 0, \end{aligned} \quad (4.12)$$

which clearly ensure the inequality “ \geq ” in (4.11). Hence, formula (4.11) is verified.

By following the subdifferential formula of support function in [35, Corollary 23.5.3], we obtain

$$\partial s_k(z) = \operatorname{argmax} \{ \langle v, z \rangle \mid \|v\|_\infty \leq 1, \|v\|_1 \leq k \}. \quad (4.13)$$

Any optimal vector $v^* \in \partial s_k(z)$ satisfies $s_k(z) - \langle v^*, z \rangle = 0$. This together with the estimates from (4.12) yields

$$v_i^* z_i \geq 0 \quad \forall i, \quad |v_i^*| = \begin{cases} 1 & \text{if } i \in T_k \\ 0 & \text{if } i \in R_k \end{cases} \quad \text{and } (k - \|v^*\|_1) |z|_{(k)} = 0. \quad (4.14)$$

If $|z|_{(k)} = 0$, then $R_k = \emptyset$. It follows from (4.14) that

$$v^* \in \left\{ v \in \mathbb{B}_\infty \mid \|v\|_1 \leq k \text{ and } v_i = \operatorname{sign}(z_i) \text{ if } i \in T_k \right\}. \quad (4.15)$$

If $|z|_{(k)} > 0$, then $\|v^*\|_1 = k$. The requirements from (4.14) tell us that

$$v^* \in \left\{ v \in \mathbb{B}_\infty \mid v_i \in \begin{cases} \{\operatorname{sign}(z_i)\} & \text{if } i \in T_k \\ \mathbb{R}_+ \operatorname{sign}(z_i) & \text{if } i \in E_k \text{ and } \sum_{i \in E_k} |v_i| = k - |T_k| \\ \{0\} & \text{if } i \in R_k \end{cases} \right\}. \quad (4.16)$$

This together with (4.15) verifies our first formula of the proposition.

To continue, observe from (4.9) and the fact that $\operatorname{par} \partial g^*(z) = \operatorname{span} N_{C_\lambda}(z)$ from Proposition 4.1 that

$$\operatorname{par} \partial g^*(z) = \operatorname{span} \left(\bigcup_{k \in A(z)} \partial s_k(z) \right) = \operatorname{span} \left(\bigcup_{k \in A(z)} \operatorname{span} \partial s_k(z) \right),$$

which verifies (4.10). Denote by $\mathcal{S}_k := \operatorname{par} \partial s_k(z) = \operatorname{aff}(\partial s_k(z) - v_k)$ for any $v_k \in \partial s_k(z)$, $k \in A(z)$. Let us construct the subspace $\operatorname{span}(v_k, \mathcal{S}_k)$ based on the two cases above:

If $|z|_{(k)} = 0$, we obtain from (4.15) that $\mathcal{S}_k = \{w \mid w_{T_k} = 0\}$, which clearly implies that

$$\operatorname{span} \partial s_k(z) = \operatorname{span} \{v_k, \mathcal{S}_k\} = \operatorname{span} \{v_k, (e_j)_{j \in E_k}\}.$$

If $|z|_{(k)} > 0$, observe from (4.16) that

$$\operatorname{aff} \partial s_k(z) = \left\{ w \mid w_{T_k} = (\operatorname{sign}(z))_{T_k}, w_{R_k} = 0, \langle w_{E_k}, (\operatorname{sign}(z))_{E_k} \rangle = k - |T_k| \right\}, \text{ and thus}$$

$$\mathcal{S}_k = \left\{ w \mid w_{T_k} = 0, w_{R_k} = 0, \langle w_{E_k}, (\operatorname{sign}(z))_{E_k} \rangle = 0 \right\}.$$

Define m_k as the largest index in E_k . It follows that

$$\operatorname{span} \partial s_k(z) = \operatorname{span} \{v_k, \mathcal{S}_k\} = \operatorname{span} \left\{ v_k, \left(e_j - \frac{\operatorname{sign}(z_j)}{\operatorname{sign}(z_{m_k})} e_{m_k} \right)_{j \in E_k \setminus \{m_k\}} \right\}.$$

The formula of $\operatorname{span} \partial s_k(z)$ in the above two cases verifies the second formula of the proposition. The proof is complete. \square

Next, we provide an explicit computation for the effective subspace $L = \operatorname{par} \partial g^*(z)$, when g is a composite convex function, which appears widely in many convex optimization models.

Proposition 4.3 (Composite functions). *Let $K : \mathbb{X} \rightarrow \mathbb{Y}$ be a linear operator between two Euclidean spaces and $h : \mathbb{Y} \rightarrow \overline{\mathbb{R}}$ be an l.s.c. polyhedral convex function with $K^{-1}(\text{dom } h) \neq \emptyset$. Define the composite function $g(x) = h(Kx)$ for $x \in \mathbb{X}$. Then for any $z \in \text{dom } g^*$, we have*

$$\text{par } \partial g^*(z) = K^{-1}(\text{par } (\partial h^*(y) \cap \text{Im } K)), \quad (4.17)$$

for any $y \in \mathbb{Y}$ satisfying

$$K^*y = z \quad \text{and} \quad g^*(z) = h^*(y). \quad (4.18)$$

Proof. Since h is a polyhedral convex function, so is h^* . Thus the Fenchel-Rockafellar conjugate formula [35, Theorem 16.3] gives us that

$$g^*(z) = \inf \{h^*(y) \mid K^*y = z\} \quad \forall y \in \mathbb{R}^n. \quad (4.19)$$

Pick any y satisfying (4.18). Note that Fenchel-Young's identity (2.6) gives rise to the following equivalences

$$\begin{aligned} x \in \partial g^*(z) &\Leftrightarrow \langle z, x \rangle = g^*(z) + g(x) \\ &\Leftrightarrow \langle K^*y, x \rangle = h^*(y) + h(Kx) \\ &\Leftrightarrow \langle y, Kx \rangle = h^*(y) + h(Kx) \\ &\Leftrightarrow Kx \in \partial h^*(y) \\ &\Leftrightarrow x \in K^{-1}(\partial h^*(y)), \end{aligned} \quad (4.20)$$

which imply that $\partial g^*(z) = K^{-1}(\partial h^*(y) \cap \text{Im } K)$. It follows that

$$\partial g^*(z) - \partial g^*(z) = K^{-1}((\partial h^*(y) \cap \text{Im } K) - (\partial h^*(y) \cap \text{Im } K)).$$

Define $A := \partial g^*(z) - \partial g^*(z)$ and $B := (\partial h^*(y) \cap \text{Im } K) - (\partial h^*(y) \cap \text{Im } K) \subset \text{Im } K$. Note from the above identity that $A = K^{-1}(B)$, i.e., $K(A) = B$. We claim next that $\text{span } A = K^{-1}(\text{span } B)$. Indeed, for any $x \in \text{span } A$, there exist $\lambda_1, \dots, \lambda_n \in \mathbb{R}$ and $x_1, \dots, x_n \in A$ such that $x = \sum_{k=1}^n \lambda_k a_k$, which yields $Kx = \sum_{k=1}^n \lambda_k K a_k \in \text{span } B$, as $K a_k \in B$. This tells us that $\text{span } A \subset K^{-1}(\text{span } B)$.

To justify the opposite inclusion, pick any $x \in K^{-1}(\text{span } B)$, i.e., $Kx \in \text{span } B$. There exist $\mu_1, \dots, \mu_m \in \mathbb{R}$ and $u_1^1, u_1^2, \dots, u_m^1, u_m^2 \in \mathbb{X}$ such that $Ku_1^1, Ku_1^2, \dots, Ku_m^1, Ku_m^2 \in \partial h^*(y)$ and that

$$Kx = \sum_{k=1}^m \mu_k (Ku_k^1 - Ku_k^2),$$

which implies that

$$x = \sum_{k=1}^m \mu_k (u_k^1 - u_k^2) + u \quad \text{for some } u \in \text{Ker } K.$$

As $0 \in B$, we have $\text{Ker } K \subset K^{-1}(B) = A$. Moreover, according to (4.20), $u_1^1, u_1^2, \dots, u_m^1, u_m^2 \in \partial g^*(z)$. It follows that $x \in \text{span } A$, i.e., $K^{-1}(\text{span } B) \subset \text{span } A$. This verifies the above claim and justifies formula (4.17). \square

Remark 4.4. In the above proposition, we suppose that h is polyhedral to be consistent with the assumption that the regularizer g is polyhedral throughout the paper. But formula (4.17) holds for other classes of functions. We just need the Fenchel-Rockafellar conjugate formula for the composite function $h(Kx)$ (4.19) to be satisfied, e.g., h is a continuous function; see also [2, Section 15.3] for other qualification conditions that make this formula valid.

A particular case of composite functions widely used in time-series signal processing and data science for computing successive differences between elements (e.g., finite differences) is the total variation below.

(iv) 1D total variation semi-norm. Let us consider the case $g(x) := \|Dx\|_1$, where D is the $(n-1) \times n$ difference matrix defined by

$$D := \begin{pmatrix} 1 & -1 & 0 & \dots & 0 \\ 0 & 1 & -1 & \dots & 0 \\ \vdots & \vdots & \ddots & \ddots & \vdots \\ 0 & 0 & \dots & 1 & -1 \end{pmatrix}_{(n-1) \times n}. \quad (4.21)$$

With $h := \|\cdot\|_1$ being the ℓ_1 norm in \mathbb{R}^{n-1} , we may write g as the composition $g(x) = h(Dx)$. Note from (4.19) that

$$g^*(z) = \inf\{\delta_{\mathbb{B}_\infty}(y) \mid D^*y = z\} = \delta_C(z)$$

where $C := \text{dom } g^* = D^*(\mathbb{B}_\infty)$. This implies that $g(x) = \sigma_C(x)$, a particular case of Proposition 4.1. However, the normal cone $N_C(z)$ may not have an explicit form. As $\text{Im } D = \mathbb{R}^{n-1}$, the parallel space of $\partial g^*(z)$, $z \in C$, is obtained from (4.17) and (4.2) by

$$\text{par } \partial g^*(z) = D^{-1}(\text{par } N_{\mathbb{B}_\infty}(y)) \quad (4.22)$$

for any $y \in \mathbb{B}_\infty$ satisfying $D^*y = z$. It follows that

$$\begin{cases} y_1 & = z_1 \\ -y_1 + y_2 & = z_2 \\ \dots & \\ -y_{n-2} + y_{n-1} & = z_{n-1} \\ y_{n-1} & = -z_n \end{cases} \iff \begin{cases} y_1 & = z_1 \\ y_2 & = z_1 + z_2 \\ \dots & \\ y_{n-1} & = z_1 + \dots + z_{n-1} \\ -y_{n-1} & = z_n \end{cases} \quad (4.23)$$

and therefore

$$\text{dom } g^* = \left\{ z \in \mathbb{R}^n \mid z_1 + \dots + z_n = 0 \text{ and } \left| \sum_{i=1}^k z_i \right| \leq 1, k = 1, \dots, n-1 \right\}.$$

From (4.22) and (4.2), we have

$$\begin{aligned} \text{par } \partial g^*(z) &= \{x \in \mathbb{R}^n \mid Dx \in \text{par } N_{\mathbb{B}_\infty}(y)\} \\ &= \{x \in \mathbb{R}^n \mid (Dx)_i = 0 \text{ if } |y_i| < 1, \text{ for } i \in \{1, \dots, n-1\}\} \\ &= \{x \in \mathbb{R}^n \mid x_i = x_{i+1} \text{ if } |y_i| < 1, \text{ for } i \in \{1, \dots, n-1\}\} \\ &= \{x \in \mathbb{R}^n \mid x_i = x_{i+1} \text{ if } |z_1 + z_2 + \dots + z_i| < 1, \text{ for } i \in \{1, \dots, n-1\}\}, \end{aligned} \quad (4.24)$$

whenever $z \in \text{dom } g^*$.

There are many more polyhedral regularizers mentioned in the Introduction that we are able to compute their effective subspaces. However, we only choose a few special cases here to support our numerical experiments in the next section.

5 Numerical experiments

In this section, we evaluate the performance of our proposed algorithms against several well-known first-order and second-order methods on both synthetic datasets and a widely used image dataset. The assessments presented here are of two types. The first type concerns performances in individual problems using synthetic datasets, measured in terms of suboptimality in the objective value $\|\varphi(x_k) - \varphi(\bar{x})\|$, the distance of the iterations to the minimizer $\|x_k - \bar{x}\|$, and the overall runtime until the stopping criterion is satisfied. We note that the optimal value $\varphi(\bar{x})$, the optimal solution \bar{x} , and the Newton direction d_k in the subproblem are all computed using the Gurobi package [17]. The second type of evaluation concerns the performance of the proposed algorithm in a real-life image processing application using the SMLM ISBI 2013 dataset [5].

For all of our numerical experiments on synthetic data, we choose the initial iterate $x_0 := 0$ and use the following *relative KKT residual* stopping criterion, suggested in [22], to determine the quality of an approximate optimal solution x_k . Specifically, we terminate the algorithms when either

$$\frac{\|x_k - \mathbf{prox}_{\alpha_k g}(x_k - A^T(Ax_k - b))\|}{1 + \|x_k\| + \|Ax_k - b\|} \leq 10^{-8}$$

or the maximum number of iterations reaches 10000. All experiments were implemented in Python (version 3.12.7) and executed on a MacBook Pro equipped with an M2 Pro CPU and 16 GB of RAM.

5.1 Least square with polyhedral regularizers

We implement a numerical experiment on synthetic data to solve the following regularized least-square optimization problems:

$$\min_{x \in \mathbb{R}^n} \frac{1}{2} \|Ax - b\|^2 + \lambda g(x), \quad \lambda > 0 \quad (5.1)$$

where the matrix A has entries generated i.i.d. from the standard Gaussian distribution $\mathcal{N}(0, 1)$, the observed signal is given by $b = Ax^* + w$ with the true signal $x^* \in \mathbb{R}^n$ and w denoting a small zero-mean additive Gaussian noise with variance σ^2 , and $g(x)$ is a regularizer that imposes prior information on the solution x^* , specified later in each experiment. Note that the effective subspaces $L = \text{par } \partial g^*(z)$ used in the following experiments are readily available in the previous section. We describe the setting for each experiment in terms of the dimension of the data matrix $A \in \mathbb{R}^{m \times n}$, the true solution $x^* \in \mathbb{R}^n$, and the tuning hyperparameters as follows:

- ℓ_1 regularizer: $(m, n) = (48, 128)$, $\|x^*\|_0 = 8$, that is, x^* has 8 nonzero elements with $\lambda_c = 0.1$, $\lambda = \lambda_c \|A^T b\|_\infty$ and noise variance $\sigma^2 = 0.001$.
- ℓ_∞ regularizer: $(m, n) = (63, 64)$, $|I_{x^*}| = 8$, where $I_{x^*} = \{i \mid |x_i^*| = \|x^*\|_\infty\}$ with $\lambda_c = 0.1$, $\lambda = \lambda_c \|A^T b\|_\infty$, and noise variance $\sigma^2 = 0.001$.
- Total variation (TV) regularizer: $(m, n) = (20, 90)$ and we generate a block-constant signal to match the TV regularizer usage for piecewise-constant structure:

$$x^* = \left(\underbrace{0.5, \dots, 0.5}_{30}, \underbrace{-0.3, \dots, -0.3}_{30}, \underbrace{0.8, \dots, 0.8}_{30} \right)^\top \in \mathbb{R}^{90}.$$

In this experiment, the tuning hyperparameters are $\lambda_c = 0.3$, $\lambda = \lambda_c \|A^T b\|_\infty$ and noise variance $\sigma^2 = 0.001$.

- OSCAR regularizer: $(m, n) = (300, 300)$. We generate a design matrix $A \in \mathbb{R}^{300 \times 300}$ whose columns i and j have covariance

$$\Sigma_{ij} := \rho^{|i-j|}, \quad \rho = 0.7.$$

We then standardize the columns of A and define the solution coefficient vector as

$$x^* = \underbrace{(0, \dots, 0)}_{0.15n}, \underbrace{(3.0, \dots, 3.0)}_{0.05n}, \underbrace{(0, \dots, 0)}_{0.25n}, \underbrace{(-4.0, \dots, -4.0)}_{0.05n}, \underbrace{(0, \dots, 0)}_{0.20n}, \underbrace{(6.0, \dots, 6.0)}_{0.05n}, \underbrace{(0, \dots, 0)}_{0.25n} \in \mathbb{R}^{300}.$$

These block-wise coefficients emulate correlated features that share identical magnitudes within each group, which is similar to the setting used in [42]. The response vector b is added with a small noise with $\sigma^2 = 0.01$. In this experiment, the tuning hyperparameters are $\lambda_c = 10^{-6}$, $\lambda_1 = \lambda_c \|A^T b\|_\infty$ and $\lambda_2 = \lambda_1$.

We compare the performance of our proposed **Algorithm 3** and **Algorithm 4** with the following first-order and second-order methods:

1. The Iterative Shrinkage-Thresholding Algorithm (ISTA) in [3].
2. The Fast Iterative Shrinkage-Thresholding Algorithm (FISTA) in [3].
3. The Semismooth Newton Augmented Lagrangian method (SSNAL) in [22].
4. The Coderivative-based Generalized Regularized Newton Method (GRNM) in [19].
5. The Globalized SCD Semismooth* Newton method (GSSN) in [13].

The update iteration x_{k+1} depends on a heuristic condition on the Euclidean distance between y_k and x_k , i.e., $\|x_k - y_k\|$. Specifically, when $\|x_k - y_k\|$ is smaller than a predefined tolerance (10^{-3} or 10^{-4} in our experiments), then $x_{k+1} = y_k - d_k$ with $d_k \in L_k$ minimizes problem (3.8), otherwise $x_{k+1} = y_k$ by skipping the Newton step (3.8). In the plots, we refer to **Algorithm 3** as Newton_ISTA and **Algorithm 4** as Newton_FISTA, respectively. Their variants with the well-known *backtracking line-search* [3] are denoted by Newton_BT_ISTA and Newton_BT_FISTA, respectively.

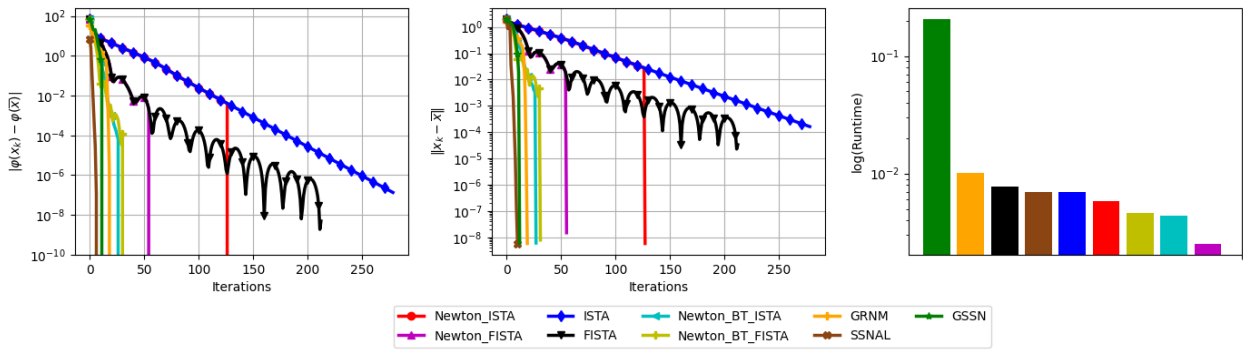


Figure 1: ℓ_1 norm

In the Lasso experiment with $g(x) = \|x\|_1$, Figure 1 demonstrates that our proposed effective subspace Newton methods, especially **Algorithm 4**, enter a quadratic local region rapidly, attaining the prescribed KKT tolerance in substantially fewer iterations and shorter wall time than ISTA

and FISTA. Compared to the coderivative-based Newton method GRNM, our method, despite exhibiting a slower decrease in the objective value per iteration, achieves faster overall runtime once the effective subspace is identified, reflecting its lower per-iteration complexity. Notably, GSSN incurs extra computational overhead from the trial backtracking loops that safeguard the forward-backward envelope decrease, see [13, Algorithm 1], which explains its longer runtime despite significant improvement per iteration. Moreover, a comparison with the semismooth Newton augmented-Lagrangian (SSNAL) solver shows that our framework attains a comparable Newton-type local convergence speed for Lasso without resorting to augmented Lagrangian subproblems, which require evaluating the generalized Jacobian of the nonsmooth proximal mapping. In contrast, our methods rely solely on explicitly computable proximal mappings, together with the parallel-subspace construction in Section 4.

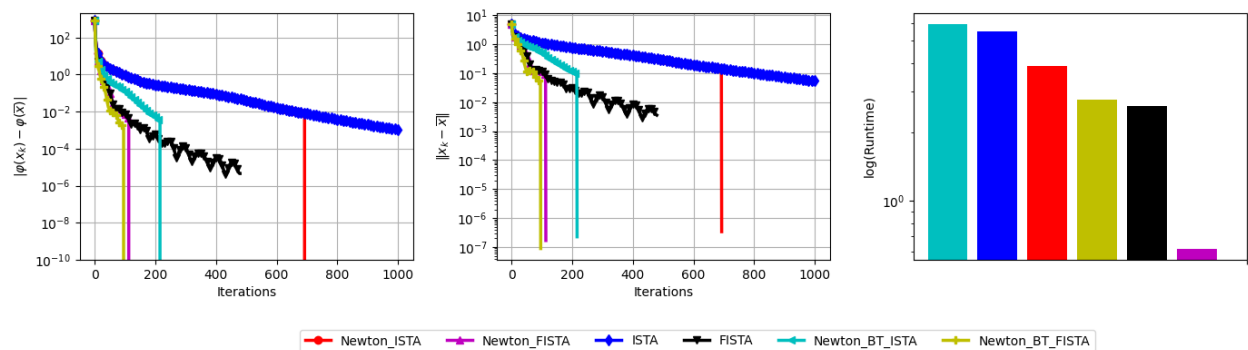


Figure 2: ℓ_∞ norm

Next, we compare the performance of our algorithm with ISTA, FISTA, and SSNAL [24] for solving the OSCAR model. We are not able to implement the GRNM and GSSN for this model.

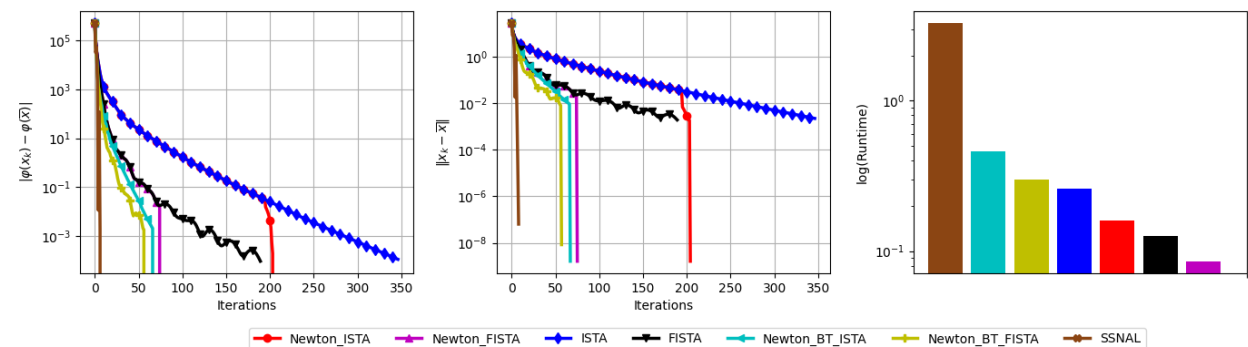


Figure 3: OSCAR regularizer

Across the ℓ_∞ , 1D total variation, and OSCAR experiments, the observed behavior is consistent with the Lasso benchmark. Our method identifies the effective structure at an early stage and subsequently exhibits the quadratic convergence profile, supporting our convergence analysis in Section 3. In all three settings, it attains the set KKT tolerance using significantly fewer iterations and reduced CPU runtime relative to standard first-order baselines, thereby outputs a high-accuracy approximate solution and avoids the extended plateaus or oscillation of first-order algorithms.

A fundamental difference between our proposed **Algorithm 3** and **Algorithm 4** and other second-order schemes is that our methods are local in nature: the quadratic convergence rate is guaranteed only when the sequence of iterates is sufficiently close to an optimal solution. Consequently, in our framework it is crucial to rely on the global convergence properties of the underlying first-order schemes. A purely heuristic switching rule that triggers a Newton step too early may cause the method to diverge. The advantage of this design is that, away from the solution, the per-iteration complexity essentially coincides with that of a first-order method, which explains the reduced computational time observed in our experiments. The trade-off is that the switching tolerance for activating the Newton step must be tuned appropriately to balance convergence speed and robustness. In contrast, GRNM, GSSN, and SSNAL are globally convergent second-order methods and therefore require more elaborate algorithmic designs and incur higher computational complexity. However, since they do not rely on any switching condition to activate the Newton step, they can be more robust in several situations.

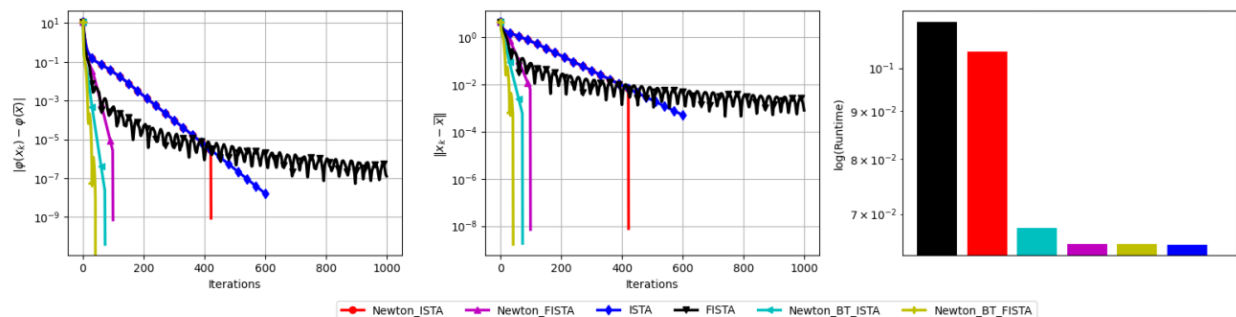


Figure 4: 1D total variation semi-norm

5.2 Sparse nonnegative image super-resolution with Poisson data

In this experiment, we address the problem of reconstructing a high-resolution nonnegative image from low-resolution Poisson-corrupted measurements, a scenario commonly encountered in fluorescence microscopy and photon-limited imaging [20, 34]. The dataset for this task is the SMLM ISBI 2013 dataset, which is composed of 361 images representing 8 tubes of 30nm diameter. The size of each image is 64×64 where each pixel is of size $100 \times 100\text{nm}$. We localize the molecules on a 256×256 pixel image corresponding to a factor $L = 4$, where the size of each pixel is thus $25 \times 25\text{nm}$. The Gaussian Point Spread Function has full width at half maximum (FWHM) equals 258.2nm . In Figure 5, we demonstrate several frames from the data set.

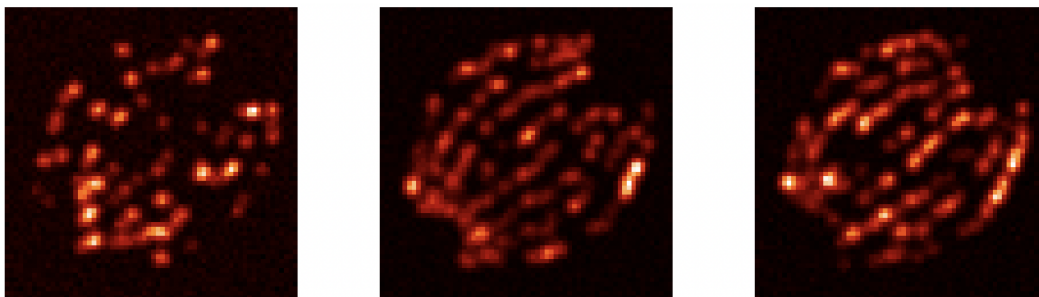


Figure 5: Images in SMLM ISBI 2013 dataset

We now describe the optimization model for the reconstruction task. Given a low-resolution and noisy observation $y \in \mathbb{R}_+^m$, we seek a sparse, nonnegative high-resolution image $x \in \mathbb{R}_+^n$ satisfying the forward process

$$y = \mathcal{P}(MHx + b),$$

where $H \in \mathbb{R}^{n \times n}$ is a known blurring/convolution operator corresponding to the point spread function (PSF), $M \in \mathbb{R}^{m \times n}$ is a downsampling operator with factor $q > 1$, $\mathcal{P}(w)$ denotes a realization of an m -dimensional Poisson random vector with mean parameter $w \in \mathbb{R}_+^m$. The vector $b \in \mathbb{R}_{>0}^m$ represents a constant background.

Following the standard Bayesian Maximum A Posteriori (MAP), one finds that the data fidelity term corresponding to the negative log-likelihood of the Poisson p.d.f. is the Kullback-Leibler (KL) divergence. Hence, the sparse nonnegative image super-resolution task can be formulated as minimizing a constrained composite optimization problem that combines a Poisson data-fidelity term, expressed via the *Kullback–Leibler (KL) divergence*, with the ℓ_1 sparsity-promoting regularizer:

$$\min_{x \geq 0} D_{\text{KL}}(y \parallel MHx + b) + \lambda \|x\|_1, \quad (5.2)$$

where $y \in \mathbb{R}_+^m$ denotes the observed photon counts and $\lambda > 0$ is a regularization parameter controlling the trade-off between data fidelity and sparsity. The KL divergence term is defined as

$$f(x) := D_{\text{KL}}(y \parallel MHx + b) = \sum_{i=1}^m \left[y_i \log \left(\frac{y_i}{(MHx)_i + b_i} \right) - y_i + (MHx)_i + b_i \right].$$

Although this function does not have full domain as required in our Theorem 3.1, its domain is an open convex set. Adapting our proof to this case is straightforward but technically involved, so we omit the details.

Note that problem (5.2) can be reformulated in the form (1.1) as an unconstrained optimization problem with the polyhedral regularizer $g(x) := \lambda \|x\|_1 + \delta_{\mathbb{R}_+^n}(x)$. Next, we briefly discuss the necessary computation steps for solving (5.2) using our proposed Newton method with effective subspaces. Firstly, the Hessian of the KL divergence admits the formulation

$$\nabla^2 f(x) = H^\top M^\top \text{Diag} \left(\frac{y}{(MHx + b)^2} \right) MH,$$

where the division and the “square” being taken element-wise. It is also locally Lipschitz continuous around any point in its domain. In addition, the proximal operator of g can be computed explicitly as the projection of the soft-thresholded point onto \mathbb{R}_+^n :

$$\mathbf{prox}_{\alpha g}(v) = P_{\mathbb{R}_+^n} \left(\mathbf{prox}_{\alpha \lambda \|\cdot\|_1}(v) \right) = \max(0, \text{sign}(v) \odot (|v| - \alpha \lambda)),$$

where \odot denotes the componentwise multiplication. The Legendre-Fenchel conjugate of $g(x)$ is

$$g^*(z) = \sup_{x \geq 0} \{ \langle z, x \rangle - \lambda \|x\|_1 \} = \sum_{i=1}^n \sup_{x_i \geq 0} (z_i - \lambda)x_i = \delta_{(-\infty, \lambda]^n}(z).$$

For any $z \in (-\infty, \lambda]^n$, denote by $I(z) := \{i \mid z_i = \lambda\}$ the active index set. The subdifferential $\partial g^*(z)$ coincides with the normal cone to the box $C = (-\infty, \lambda]^n$, which has the representation

$$N_C(z) = \{v \in \mathbb{R}^n \mid v_i \geq 0 \text{ if } z_i = \lambda, v_i = 0 \text{ if } z_i < \lambda\} = \{v \in \mathbb{R}^n \mid v_{I(z)} \geq 0, v_{I(z)^c} = 0\}.$$

The corresponding effective subspace, which defines the constraint in the Newton step, is obtained easily as

$$\text{par } \partial g^*(z) = N_C(z) - N_C(z) = \mathbb{R}^{I(z)} \times \{0\}^{I(z)^c}.$$

In this experiment, the starting iteration is $x_0 = H^\top M^\top y$ and the tuning hyperparameter is $\lambda = 0.5 \|\max\{\nabla f(0), 0\}\|_\infty$. Since the gradient ∇f is not globally Lipschitz continuous, to the best of our knowledge there is no solid theoretical guarantee for using ISTA or FISTA with a constant stepsize $\alpha > 0$, especially concerning the convergence rate. However, ∇f is still locally Lipschitz continuous, and thus, when equipped with a backtracking line-search, both ISTA and FISTA schemes converge [4]. The reconstruction results are illustrated in Figure 6, in which the proposed **Algorithm 4** with backtracking line-search successfully recovers fine structural details of the image.

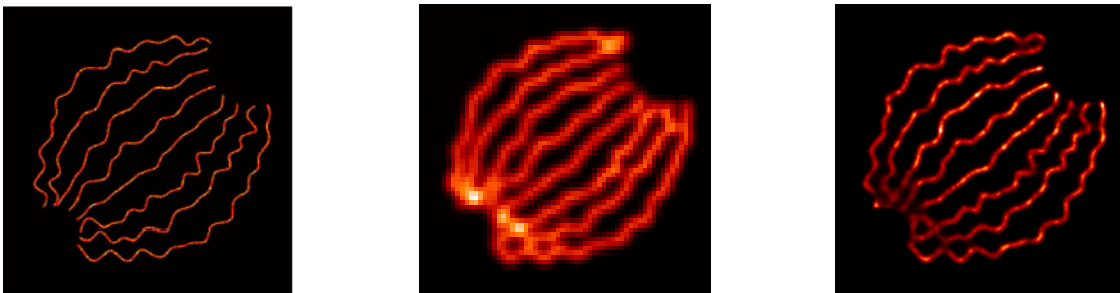


Figure 6: From left to right: High-resolution ground truth, Mean of original frames, Mean of reconstructed frames using **Algorithm 4** with backtracking line-search.

6 Conclusion

In this paper, we introduce a Newton-type method for nonsmooth composite optimization that leverages tilt-stability and effective subspace identification to achieve local quadratic convergence. Our approach departs from existing manifold Newton methods and can be viewed as a particular case of coderivative-based and SCD Newton methods, while avoiding the computation of sophisticated second-order structures. In particular, we provide constructive characterizations of the effective subspaces for a wide family of polyhedral regularizers, including the ℓ_1 norm, the ℓ_∞ norm, the sorted ℓ_1 norm, and the 1D total variation semi-norm. Numerical experiments confirm the practical efficiency of the proposed method, demonstrating a significant acceleration over first-order schemes and a competitive performance relative to other Newton-type approaches.

Several directions remain open for future research. Extending our approach to non-polyhedral structured regularizers such as the nuclear norm, group-sparsity with overlapping blocks, and the isotropic total variation would broaden the scope of applicability. Although the technique in our main Theorem 3.1 heavily relies on properties of polyhedral mapping, we believe that the strategy used in this paper can handle the non-polyhedral cases with some modifications. Moreover, our approach can be extended to solving the generalized equation in the format

$$0 \in F(x) + \partial g(x), \tag{6.1}$$

in which $F : \mathbb{X} \rightarrow \mathbb{X}$ is a continuously differentiable (not necessarily monotone) mapping and g is a polyhedral mapping. In this case, the tilt-stability assumption at the minimizer \bar{x} of (3.1) can be relaxed and replaced with the *metric regularity* of the mapping $(F + \partial g)$ at a solution \bar{x} of (6.1)

for 0. This is a research in progress with potential applications to different and broader classes of optimization problems.

Acknowledgments

We are deeply grateful to C. Wylie for kindly sharing his code implementation of the Newton method with active manifolds combined with FISTA, as developed in [41], during the development of this paper.

References

- [1] G. Bareilles, F. Iutzeler, and J. Malick. Newton acceleration on manifolds identified by proximal gradient methods. *Mathematical Programming*, 200:37–70, 2023.
- [2] H. H. Bauschke and P. L. Combettes. *Convex Analysis and Monotone Operator Theory in Hilbert Spaces*. CMS Books in Mathematics. Springer, Cham, Switzerland, 2nd edition, 2017.
- [3] A. Beck and M. Teboulle. A fast iterative shrinkage-thresholding algorithm for linear inverse problems. *SIAM Journal on Imaging Sciences*, 2(1):183–202, 2009.
- [4] J. Y. Bello Cruz and T. T. A. Nghia. On the convergence of the forward–backward splitting method with linesearches. *Optimization Methods and Software*, 31(6):1209–1238, 2016.
- [5] Biomedical Imaging Group, EPFL. 2013 isbi grand challenge: Localization microscopy. <http://bigwww.epfl.ch/smlm/challenge2013/index.html>, 2013.
- [6] H. D. Bondell and B. J. Reich. Simultaneous regression shrinkage, variable selection and clustering of predictors with OSCAR. *Biometrics*, 64(1):115–123, 2008.
- [7] S. Boyd, N. Parikh, E. Chu, B. Peleato, and J. Eckstein. Distributed optimization and statistical learning via the alternating direction method of multipliers. *Foundations and Trends® in Machine learning*, 3(1):1–122, 2011.
- [8] A. Chambolle and C. Dossal. On the convergence of the iterates of the “Fast Iterative Shrinkage/Thresholding Algorithm”. *Journal of Optimization Theory and Applications*, 166(3):968–982, 2015.
- [9] A. Chambolle and T. Pock. A first-order primal-dual algorithm for convex problems with applications to imaging. *Journal of Mathematical Imaging and Vision*, 40(1):120–145, 2011.
- [10] Y. Cui, T. Hoheisel, T. T. A. Nghia, and D. Sun. Lipschitz stability of least-squares problems regularized by functions with \mathcal{C}^2 -cone reducible conjugates. *arXiv:2409.13118*, 2024.
- [11] A. L. Dontchev and R. T. Rockafellar. *Implicit Functions and Solution Mappings: A View from Variational Analysis*. Springer Series in Operations Research and Financial Engineering. Springer, New York, 2nd edition, 2014.
- [12] F. Facchinei and J.-S. Pang. *Finite-Dimensional Variational Inequalities and Complementarity Problems*. Springer, New York, 2003.
- [13] H. Gfrerer. On a globally convergent semismooth* Newton method in nonsmooth nonconvex optimization. *Computational Optimization and Applications*, 91:67–124, 2025.
- [14] H. Gfrerer, S. Hubmer, and R. Ramlau. On SCD semismooth* Newton methods for the efficient minimization of Tikhonov functionals with non-smooth and non-convex penalties. *Inverse Problems*, 41:075002, 2025.
- [15] H. Gfrerer and J. V. Outrata. On a semismooth* Newton method for solving generalized equations. *SIAM Journal on Optimization*, 31:489–517, 2021.

- [16] H. Gfrerer and J. V. Outrata. On (local) analysis of multifunctions via subspaces contained in graphs of generalized derivatives. *Journal of Mathematical Analysis and Applications*, 508:125895, 2022.
- [17] Gurobi Optimization, LLC. Gurobi Optimizer Reference Manual, 2024.
- [18] P. D. Khanh, B. S. Mordukhovich, and V. T. Phat. Coderivative-based Newton methods in structured nonconvex and nonsmooth optimization. *arXiv:2403.04262*, 2025.
- [19] P. D. Khanh, B. S. Mordukhovich, V. T. Phat, and D. B. Tran. Globally convergent coderivative-based generalized Newton methods in nonsmooth optimization. *Mathematical Programming*, 205:373–429, 2024.
- [20] M. Lazzaretti, S. Rebegoldi, L. Calatroni, and C. Estatico. A scaled and adaptive FISTA algorithm for signal-dependent sparse image super-resolution problems. In *Scale Space and Variational Methods in Computer Vision*, Lecture Notes in Computer Science, pages 242–253, Cham, 2021. Springer International Publishing.
- [21] A. S. Lewis and C. J. S. Wylie. Active-set Newton methods and partial smoothness. *Mathematics of Operations Research*, 46(2):712–725, 2021.
- [22] X. Li, D. Sun, and K.-C. Toh. A highly efficient semismooth Newton augmented Lagrangian method for solving Lasso problems. *SIAM Journal on Optimization*, 28(1):433–458, 2018.
- [23] J. Liang, T. Luo, and C.-B. Schönlieb. Improving “Fast Iterative Shrinkage-Thresholding Algorithm”: Faster, smarter, and greedier. *SIAM Journal on Scientific Computing*, 44(3):A1069–A1091, 2022.
- [24] Z. Luo, D. Sun, K.-C. Toh, and N. Xiu. Solving the OSCAR and SLOPE models using a semismooth Newton-based augmented Lagrangian method. *Journal of Machine Learning Research*, 20:1–25, 2019.
- [25] R. Mifflin. Semismooth and semiconvex functions in constrained optimization. *SIAM Journal on Control and Optimization*, 15(6):959–972, 1977.
- [26] B. Mordukhovich. *Second-Order Variational Analysis in Optimization, Variational Stability, and Control: Theory, Algorithms, Applications*. Springer, Cham, Switzerland, 2024.
- [27] B. S. Mordukhovich. Sensitivity analysis in nonsmooth optimization. In D. A. Field and V. Komkov, editors, *Theoretical Aspects of Industrial Design*, pages 32–46. SIAM, Philadelphia, 1992.
- [28] B. S. Mordukhovich. *Variational Analysis and Generalized Differentiation*. Springer, 2006.
- [29] B. S. Mordukhovich and T. T. A. Nghia. Second-order characterizations of tilt stability with applications to nonlinear programming. *Mathematical Programming*, 149(1–2):83–104, 2015.
- [30] B. S. Mordukhovich and R. T. Rockafellar. Second-order subdifferential calculus with applications to tilt stability in optimization. *SIAM Journal on Optimization*, 22(3):953–986, 2012.
- [31] B. S. Mordukhovich and E. Sarabi. Generalized Newton algorithms for tilt-stable minimizers in nonsmooth optimization. *SIAM Journal on Optimization*, 31:1184–1214, 2021.
- [32] R. A. Poliquin and R. T. Rockafellar. Tilt stability of a local minimum. *SIAM Journal on Optimization*, 8(2):287–299, 1998.
- [33] L. Qi and J. Sun. A nonsmooth version of Newton’s method. *Mathematical Programming*, 58(1–3):353–367, 1993.
- [34] S. Rebegoldi and L. Calatroni. Scaled, inexact, and adaptive generalized FISTA for strongly convex optimization. *SIAM Journal on Optimization*, 32(3):2428–2459, 2022.
- [35] R. T. Rockafellar. *Convex Analysis*. Princeton University Press, Princeton, 1970.
- [36] R. T. Rockafellar and R. J.-B. Wets. *Variational Analysis*. Springer Science & Business Media, 2009.
- [37] Y. She. Sparse regression with exact clustering. *Electronic Journal of Statistics*, 4:1055–1096, 2010.
- [38] R. Tibshirani. Regression shrinkage and selection via the Lasso. *Journal of the Royal Statistical Society: Series B (Statistical Methodology)*, 58:267–288, 1996.

- [39] R. Tibshirani, M. Saunders, S. Rosset, J. Zhu, and K. Knight. Sparsity and smoothness via the fused Lasso. *Journal of the Royal Statistical Society: Series B (Statistical Methodology)*, 67(1):91–108, 2005.
- [40] Y. S. Wu, X. Shen, and C. J. Geyer. Adaptive regularization using the entire solution surface. *Biometrika*, 96(3):513–527, 2009.
- [41] C. J. S. Wylie. *Partly Smooth Models and Algorithms*. PhD thesis, Cornell University, Ithaca, NY, Dec. 2019.
- [42] X. Zeng and M. A. T. Figueiredo. The ordered weighted ℓ_1 norm: Atomic formulation, dual norm, and projections. *arXiv:1409.4271*, 2014.